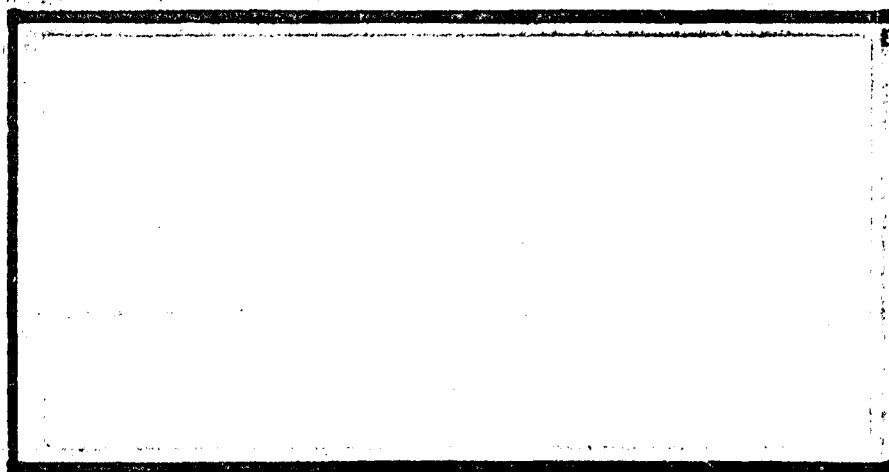
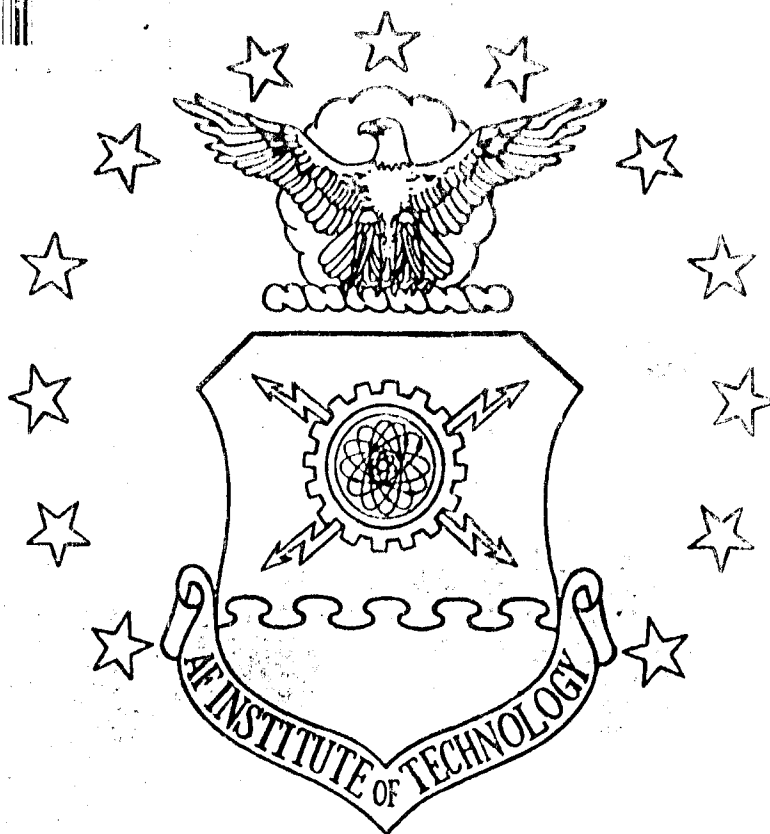


AD-A238 682



**DISTRIBUTION STATEMENT A**

Approved for public release  
Distribution Unlimited

DEPARTMENT OF THE AIR FORCE  
AIR UNIVERSITY

**AIR FORCE INSTITUTE OF TECHNOLOGY**

Wright-Patterson Air Force Base, Ohio

DTIC  
ELECTE  
JUL 23 1991

S D D

AFIT/ENP/GNE/91M-9

6

DTIC  
ELECTE  
JUL 23 1991  
S D D

AN ASSESSMENT OF THE ACCURACY  
OF SEMI-EMPIRICAL QUANTUM  
CHEMISTRY CALCULATIONS OF THE  
MECHANICAL PROPERTIES OF  
POLYMERS

THESIS

JAMES R. SHOEMAKER, Captain USAF  
AFIT/ENP/GNE/91M-9

DISTRIBUTION STATEMENT A  
Approved for public release  
Distribution Unlimited

91-05742



91 7 19 7 71

AFIT/ENP/GNE/91M-9

AN ASSESSMENT OF THE ACCURACY OF  
SEMI-EMPIRICAL QUANTUM CHEMISTRY  
CALCULATIONS OF THE  
MECHANICAL PROPERTIES OF POLYMERS

THESIS

Presented to the faculty of the School of Engineering  
of the Air Force Institute of Technology

Air University

In Partial Fulfillment of the  
Requirements for the Degree of  
Master of Science in Nuclear Science

James R. Shoemaker, B. S.  
Captain, USAF

March 1991

Accession For	
NTIS CRASH	✓
DTIC	✓
AD	✓
AN	✓
AS	✓
AT	✓
AV	✓
AW	✓
AX	✓
AY	✓
BA	✓
BB	✓
BC	✓
BD	✓
BE	✓
BF	✓
BG	✓
BH	✓
BI	✓
BJ	✓
BK	✓
BL	✓
BM	✓
BN	✓
BO	✓
BP	✓
BQ	✓
BR	✓
BS	✓
BT	✓
BU	✓
BV	✓
BW	✓
BX	✓
BY	✓
CA	✓
CB	✓
CC	✓
CD	✓
CE	✓
CF	✓
CG	✓
CH	✓
CI	✓
CJ	✓
CK	✓
CL	✓
CM	✓
CN	✓
CO	✓
CP	✓
CQ	✓
CR	✓
CS	✓
CT	✓
CU	✓
CV	✓
CW	✓
CX	✓
CY	✓
DA	✓
DB	✓
DC	✓
DD	✓
DE	✓
DF	✓
DG	✓
DH	✓
DI	✓
DJ	✓
DK	✓
DL	✓
DM	✓
DN	✓
DO	✓
DP	✓
DQ	✓
DR	✓
DS	✓
DT	✓
DU	✓
DV	✓
DW	✓
DX	✓
DY	✓
EA	✓
EB	✓
EC	✓
ED	✓
EE	✓
EF	✓
EG	✓
EH	✓
EI	✓
EJ	✓
EK	✓
EL	✓
EM	✓
EN	✓
EO	✓
EP	✓
EQ	✓
ER	✓
ES	✓
ET	✓
EU	✓
EV	✓
EW	✓
EX	✓
EY	✓
FA	✓
FB	✓
FC	✓
FD	✓
FE	✓
FF	✓
FG	✓
FH	✓
FI	✓
FJ	✓
FK	✓
FL	✓
FM	✓
FN	✓
FO	✓
FP	✓
FQ	✓
FR	✓
FS	✓
FT	✓
FU	✓
FV	✓
FW	✓
FX	✓
FY	✓
GA	✓
GB	✓
GC	✓
GD	✓
GE	✓
GF	✓
GG	✓
GH	✓
GI	✓
GJ	✓
GK	✓
GL	✓
GM	✓
GN	✓
GO	✓
GP	✓
GQ	✓
GR	✓
GS	✓
GT	✓
GU	✓
GV	✓
GW	✓
GX	✓
GY	✓
HA	✓
HB	✓
HC	✓
HD	✓
HE	✓
HF	✓
HG	✓
HH	✓
HI	✓
HJ	✓
HK	✓
HL	✓
HM	✓
HN	✓
HO	✓
HP	✓
HQ	✓
HR	✓
HS	✓
HT	✓
HU	✓
HV	✓
HW	✓
HX	✓
HY	✓
IA	✓
IB	✓
IC	✓
ID	✓
IE	✓
IF	✓
IG	✓
IH	✓
II	✓
IJ	✓
IK	✓
IL	✓
IM	✓
IN	✓
IO	✓
IP	✓
IQ	✓
IR	✓
IS	✓
IT	✓
IU	✓
IV	✓
IW	✓
IX	✓
IY	✓
JA	✓
JB	✓
JC	✓
JD	✓
JE	✓
JF	✓
JG	✓
JH	✓
JI	✓
JJ	✓
JK	✓
JL	✓
JM	✓
JN	✓
JO	✓
JP	✓
JQ	✓
JR	✓
JS	✓
JT	✓
JU	✓
JV	✓
JW	✓
JX	✓
JY	✓
KA	✓
KB	✓
KC	✓
KD	✓
KE	✓
KF	✓
KG	✓
KH	✓
KI	✓
KJ	✓
KK	✓
KL	✓
KM	✓
KN	✓
KO	✓
KP	✓
KQ	✓
KR	✓
KS	✓
KT	✓
KU	✓
KV	✓
KW	✓
KX	✓
KY	✓
LA	✓
LB	✓
LC	✓
LD	✓
LE	✓
LF	✓
LG	✓
LH	✓
LI	✓
LJ	✓
LK	✓
LL	✓
LM	✓
LN	✓
LO	✓
LP	✓
LQ	✓
LR	✓
LS	✓
LT	✓
LU	✓
LV	✓
LW	✓
LX	✓
LY	✓
MA	✓
MB	✓
MC	✓
MD	✓
ME	✓
MF	✓
MG	✓
MH	✓
MI	✓
MJ	✓
MK	✓
ML	✓
MM	✓
MN	✓
MO	✓
MP	✓
MQ	✓
MR	✓
MS	✓
MT	✓
MU	✓
MV	✓
MW	✓
MX	✓
MY	✓
NA	✓
NB	✓
NC	✓
ND	✓
NE	✓
NF	✓
NG	✓
NH	✓
NI	✓
NJ	✓
NK	✓
NL	✓
NM	✓
NN	✓
NO	✓
NP	✓
NQ	✓
NR	✓
NS	✓
NT	✓
NU	✓
NV	✓
NW	✓
NX	✓
NY	✓
OA	✓
OB	✓
OC	✓
OD	✓
OE	✓
OF	✓
OG	✓
OH	✓
OI	✓
OJ	✓
OK	✓
OL	✓
OM	✓
ON	✓
OO	✓
OP	✓
OQ	✓
OR	✓
OS	✓
OT	✓
OU	✓
OV	✓
OW	✓
OX	✓
OY	✓
PA	✓
PB	✓
PC	✓
PD	✓
PE	✓
PF	✓
PG	✓
PH	✓
PI	✓
PJ	✓
PK	✓
PL	✓
PM	✓
PN	✓
PO	✓
PP	✓
PQ	✓
PR	✓
PS	✓
PT	✓
PU	✓
PV	✓
PW	✓
PX	✓
PY	✓
QA	✓
QB	✓
QC	✓
QD	✓
QE	✓
QF	✓
QG	✓
QH	✓
QI	✓
QJ	✓
QK	✓
QL	✓
QM	✓
QN	✓
QO	✓
QP	✓
QQ	✓
QR	✓
QS	✓
QT	✓
QU	✓
QV	✓
QW	✓
QX	✓
QY	✓
RA	✓
RB	✓
RC	✓
RD	✓
RE	✓
RF	✓
RG	✓
RH	✓
RI	✓
RJ	✓
RK	✓
RL	✓
RM	✓
RN	✓
RO	✓
RP	✓
RQ	✓
RR	✓
RS	✓
RT	✓
RU	✓
RV	✓
RW	✓
RX	✓
RY	✓
SA	✓
SB	✓
SC	✓
SD	✓
SE	✓
SF	✓
SG	✓
SH	✓
SI	✓
SJ	✓
SK	✓
SL	✓
SM	✓
SN	✓
SO	✓
SP	✓
SQ	✓
SR	✓
SS	✓
ST	✓
SU	✓
SV	✓
SW	✓
SX	✓
SY	✓
TA	✓
TB	✓
TC	✓
TD	✓
TE	✓
TF	✓
TG	✓
TH	✓
TI	✓
TJ	✓
TK	✓
TL	✓
TM	✓
TN	✓
TO	✓
TP	✓
TQ	✓
TR	✓
TS	✓
TT	✓
TU	✓
TV	✓
TW	✓
TX	✓
TY	✓
UA	✓
UB	✓
UC	✓
UD	✓
UE	✓
UF	✓
UG	✓
UH	✓
UI	✓
UJ	✓
UK	✓
UL	✓
UM	✓
UN	✓
UO	✓
UP	✓
UQ	✓
UR	✓
US	✓
UT	✓
UU	✓
UV	✓
UW	✓
UX	✓
UY	✓
VA	✓
VB	✓
VC	✓
VD	✓
VE	✓
VF	✓
VG	✓
VH	✓
VI	✓
VJ	✓
VK	✓
VL	✓
VM	✓
VN	✓
VO	✓
VP	✓
VQ	✓
VR	✓
VS	✓
VT	✓
VU	✓
VV	✓
VW	✓
VX	✓
VY	✓
WA	✓
WB	✓
WC	✓
WD	✓
WE	✓
WF	✓
WG	✓
WH	✓
WI	✓
WJ	✓
WK	✓
WL	✓
WM	✓
WN	✓
WO	✓
WP	✓
WQ	✓
WR	✓
WS	✓
WT	✓
WU	✓
WV	✓
WW	✓
WX	✓
WY	✓
XA	✓
XB	✓
XC	✓
XD	✓
XE	✓
XF	✓
XG	✓
XH	✓
XI	✓
XJ	✓
XK	✓
XL	✓
XM	✓
XN	✓
XO	✓
XP	✓
XQ	✓
XR	✓
XS	✓
XT	✓
XU	✓
XV	✓
XW	✓
XX	✓
XY	✓
YA	✓
YB	✓
YC	✓
YD	✓
YE	✓
YF	✓
YG	✓
YH	✓
YI	✓
YJ	✓
YK	✓
YL	✓
YM	✓
YN	✓
YO	✓
YP	✓
YQ	✓
YR	✓
YS	✓
YT	✓
YU	✓
YV	✓
YW	✓
YX	✓
YI	✓
ZA	✓
ZB	✓
ZC	✓
ZD	✓
ZE	✓
ZF	✓
ZG	✓
ZH	✓
ZI	✓
ZJ	✓
ZK	✓
ZL	✓
ZM	✓
ZN	✓
ZO	✓
ZP	✓
ZQ	✓
ZR	✓
ZS	✓
ZT	✓
ZU	✓
ZV	✓
ZW	✓
ZX	✓
ZY	✓

Approved for public release; distribution unlimited.

## Acknowledgements

I would like to acknowledge the support of the Polymer Branch of the Wright Laboratory's Material Directorate in providing me access to the Silicon Graphics workstation on which the bulk of the calculations in my thesis were performed. I would like to thank the members of the Plasma Physics Group of the Aero Propulsion and Power Directorate, Alan, Charlie, Bish, Bob, Jerry, and Jimmy, for their encouragement and support throughout my thesis and the time before when I actually did something useful for a living, and providing me with the opportunity to still do some science during my term at AFIT. I'd like to thank my advisor, Captain Pete (v=42) Haaland for giving me a great deal of flexibility in this thesis, Wade Adams for trying to ground all this high-falutin' theory into something useful, Doug Dudis for his advice on running the computations, and Mike Sabochick for his sanity check (sorry Mike, insanity is more fun). I'd like to thank Bob Young for suggesting polydiacetylene as a benchmark polymer, and Jimmy Stewart for his help in using MOPAC. And of course, to put the blame squarely where it should lie, I'd like to thank my parents for letting me stay up past my bedtime to watch every U. S. space shot letting me hope that I could do something neat like that some day.

## Table of Contents

	Page
Acknowledgements . . . . .	ii
List of Figures . . . . .	iv
List of Tables . . . . .	vi
Abstract . . . . .	vii
I. Introduction . . . . .	1
II. Approximate Molecular Structure Calculations . . . . .	8
Ab-Initio Method . . . . .	8
Semi-Empirical Method . . . . .	14
III. Relationship of Theory to Experiment . . . . .	22
Calculations of Mechanical Properties . . . . .	22
Measurement of Polymer Modulus . . . . .	29
IV. Polyethylene Results and Discussion . . . . .	34
Molecular Structure and Modulus Calculation . . . . .	34
Comparisons with Spectroscopy . . . . .	46
V. Polydiacetylene Results and Discussion . . . . .	60
Substituent Effects . . . . .	60
Molecular Structure . . . . .	64
Modulus Calculations . . . . .	70
Comparisons with Spectroscopy . . . . .	74
VI. Summary, Conclusions, and Recommendations . . . . .	84
References . . . . .	90
Vita . . . . .	93

## List of Figures

Figure	Page
1. Flow charts of ab-initio and semi-empirical calculations . . . . .	16
2. General polymer stress-strain curve . . . . .	23
3. Comparison of Morse and harmonic potentials . . . . .	27
4. Comparison of amorphous and idealized polymer structures . . . . .	30
5. Comparison of ab initio and semi-empirical structure calculations of a PE oligomer . . . . .	35
6. PE cluster strain dependent heat of formation potential . . . . .	36
7. Comparison of second derivatives of PE heat of formation potential . . .	39
8. Distribution of strain in a PE cluster as a function of <i>c</i> axis strain . . .	41
9. Comparison of PE cluster strain potentials, constrained versus unconstrained . . . . .	42
10. Crystal structure of PE. . . . .	44
11. PE crystal strain dependent diffraction response . . . . .	45
12. Comparison of calculated and experimental strain dependent PE spectral shifts, Raman active asymmetric C-C stretch . . . . .	52
13. Comparison of calculated and experimental strain dependent PE spectral shifts, Raman active symmetric C-C stretch . . . . .	53
14. Comparison of Morse and AM1 C-C strain potentials. . . . .	56
15. Comparison of Morse and AM1 C-C strain potentials, expanded view about equilibrium. . . . .	57
16. PDA backbone structure. . . . .	61
17. Comparisons of ab-initio and semi-empirical calculations of PDA structure. . . . .	67
18. Distribution of strain in a PDA cluster as a function of <i>c</i> axis strain . .	69
19. Substituent effect on PDA strain dependent heat of formation . . . . .	71

20. PDA oligomer used in strain calculations . . . . .	73
21. Normal coordinates of the PDA vibrational frequencies used for comparisons to semi-empirical calculations . . . . .	76
22. Strain dependent spectral shifts of the PDA vibrational mode shown in figure 21a . . . . .	78
23. Strain dependent spectral shifts of the PDA vibrations mode shown in figure 21b. . . . .	80
24. Comparison of PDA C-C bond potentials . . . . .	81
25. Comparison of the behavior of Morse, harmonic, and cubic bond potentials and their derivatives under strain. . . . .	87

## List of Tables

Table	Page
1. Summary of Calculations Performed . . . . .	6
2. Average Molecular Structure Geometry Errors in AM1. . . . .	20
3. Comparison of Experimental, Molecular Mechanics, Semi-Empirical, and Ab-Initio Frequencies for a PE Oligomer . . . . .	48
4. PDA Derivative Modulus Comparison . . . . .	62
5. PDA Cluster Series Calculations . . . . .	65
6. PDA Oligomer Series Calculations. . . . .	65
7. PDA Calculated and Measured Modulus Comparison. . . . .	72
8. PDA Calculated and Spectroscopically Derived Force Constants. . . . .	83



Abstract

The ultimate mechanical properties of polymers, assuming perfect morphology, will be limited by the mechanical properties of a single, ideal polymer chain. Previous calculations of polymer chain moduli using semi-empirical (SE) quantum chemistry methods have resulted in modulus values much higher than experimentally measured. This study investigated the error in the calculated inherent to the method of calculation by comparing SE results for C-C bond potentials in two well characterized polymers, polyethylene and polydiacetylene. It was found that the SE calculation systematically overpredicted bond stiffness in these polymers by approximately 25% to 30%. This is the upper limit on the modulus overprediction, depending on the importance of bond extension/compression (as compared to other deformation modes) in the overall deformation of the polymer chain. It is believed that this discrepancy is caused in part by the omission of bond stiffness information in the parameterization of the SE method, and in part by the omission of electron correlation in the calculation (Hartree-Fock Limit).

## I INTRODUCTION

The wave mechanics formulation of quantum theory derived by Erwin Schrodinger in 1926 satisfied the three fundamental requirements of a good scientific theory: agreement with and explanation of existing experimental data, and prediction of phenomena which were confirmed in subsequent experiments. The power of wave mechanics is tempered by its fundamental limitation, that analytic solutions for wave functions and energies can only be obtained for atoms with symmetric, central Coulomb potentials, namely atomic hydrogen (and one-electron ions). One could argue that being able to describe over 99% of the known matter in the universe is sufficient. However, since the remaining 1% includes 6-electron atom based humans who breathe 18-electron molecules, there was sufficient motivation to develop approximate methods to extend Schrodinger's theory to multi-electron systems.

We'll consider two quantum-based approximations, both of which rely on the Hartree-Fock / self consistent field (SCF) method. The ab-initio implementation of the SCF makes few simplifying assumptions, and provides the best agreement with experiment. However, ab-initio methods are computationally expensive and impractical for all but fairly simple systems (roughly fewer than 10 non-hydrogen atoms) even on current state-of-the-art supercomputers. Another implementation of the SCF method is called the semi-empirical (SE) approach because it relies partly on experimental data from atomic spectra. The main difference between ab-initio and SE methods is that some of the electron-electron interaction

integrals are replaced by a set of parameters which have been selected to provide the best agreement (minimum least squares error) to equilibrium molecular properties of some large set of test compounds. SE results have poorer agreement with experiment than ab-initio results, but the parameterization decreases the computational cost so that larger systems (up to approximately 50 non-hydrogen atoms) can be readily calculated. However, SE methods are limited to those elements which have been parameterized. A third method, known as molecular mechanics, is based on classical mechanics and has been used on very large systems (up to 100,000 non-hydrogen atoms). Application of molecular mechanics is limited to situations where system-specific interaction potentials, usually atom-pair potentials, have been measured. Although this is a non quantum-based method, molecular mechanics provides excellent agreement with experiment because the measured potentials represent the net result of all the physical processes involved, however small (i.e., makes no approximations). The accuracy of the results depends directly on the experimental accuracy. These three approaches are complementary, providing access to different (not orthogonal) parameter spaces.

The semi-empirical method has recently been applied to calculate mechanical properties of polymers away from equilibrium<sup>1,2</sup>. In these calculations, an infinite, ideal polymer is simulated by calculating a molecule composed of one or more monomer repeat units (a cluster) specified with periodic boundary conditions. The number of repeat units in the cluster is determined by the conjugation length in the polymer, i.e., the

cluster must be long enough so that its ends are electronically isolated. The minimum energy geometry of the cluster is calculated, with the overall cluster length specified as a variable which is optimized. This length is increased ( or decreased) and then held fixed, and the rest of the cluster geometry is optimized under this constraint. The minimum heat of formation of the cluster is calculated for a range of cluster lengths, generating a restoring potential for the cluster. The second derivative of this potential is the effective force constant for the cluster, from which the polymer Young's modulus, stiffness per unit area, can be calculated. The modulus values calculated using this procedure are significantly higher than experimental measurement. There are two possible reasons for this result: measurements are made on bulk materials, which deviate from the ideal structure simulated in the calculations (ultimate modulus vs. practical modulus), and/or the semi-empirical method parameters are not valid away from the conditions for which they were derived.

The goal of this thesis is to perform a critical assessment of the applicability of the semi-empirical (SE) quantum approximation for the calculation of polymer mechanical properties away from equilibrium, and to bound the accuracy of the calculation of molecular bond stiffnesses at equilibrium. The non-experimental parameters used in the SE methods are obtained by adjusting a set of initial estimates of the parameters for each element to minimize the least squares error in reproducing various molecular properties. In the approximation used in this study, the parameters were optimized to reproduce gas-phase, equilibrium, 297 K

values of heats of formation, dipole moments, ionization potentials, and molecular geometries, none of which depend sensitively on the derivatives of the intra-molecular potentials. The modulus calculation involves a series of SE calculations in which one parameter, the length of the cluster along the polymer axis, is fixed at non-equilibrium values. All other cluster properties, bond angles, bond lengths, are adjusted away from their equilibrium values to minimize the heat of formation under this constraint. Hence the modulus calculation involves extrapolations of non-equilibrium properties based on equilibrium data which provide no guidance for the direction this extrapolation, i.e., derivatives of the intra-molecular potentials. Therefore, the range of displacements away from equilibrium for which SE calculations may be accurate is undefined. The equilibrium bond stiffness is the second derivative of the bond potential at the equilibrium bond length. These data were not used to anchor the SE parameterization, thus the accuracy of bond stiffnesses predicted by a SE calculation requires investigation.

This assessment of the SE approach will be performed by comparing calculated and observed properties of polyethylene (PE) and polydiacetylene (PDA). These polymers were selected because they possess simple backbone structures, both have been well characterized experimentally, and they can be made in crystalline form which removes much of the morphological uncertainty in comparing the experimental results to the calculations. Real polymers are at best semi-ordered, have a random chain orientation, and have structural defects; these characteristics limit bulk mechanical

strength and modulus rather than the inherent chain properties.

The specific properties for which comparisons will be made are summarized in Table 1. Each property provides a different level of comparison with the SE method. The equilibrium geometry is one of the four properties against which the SE method was compared and gives an indication of the baseline error involved. Because polymer modulus is the net result of many deformations in the repeat unit (bond extension, bond angle bending, torsion angle twisting), modulus alone is not a sensitive test of the SE method. In order to determine the effect of the SE method on the calculated modulus, one must compare SE predictions for specific components within the repeat unit with experiment. In order to obtain information on specific bonds within the molecule, one needs to examine spectroscopic data, the energy shift of Raman and IR active lines as a function of strain. Spectroscopy provides information on second and third derivatives of bond potentials generated by the SE parameterization, which describe the bond strength. In this study, comparisons will concentrate on backbone vibrational modes of PE and PDA which show the largest strain sensitivity. The strain-dependent intra-molecular potentials calculated by the SE method will be directly compared with empirical Morse potentials that have been shown to agree with the spectroscopic data on the polymers.

TABLE 1  
SUMMARY OF COMPARISONS

<u>PROPERTY</u>	<u>PE</u>	<u>PDA</u>
Equilibrium Geometry		
Crystallographic Results	*	*
Ab-Initio Calculation	*	*
Substituent Effect		*
Modulus		
Bulk Measurements	*	*
X-Ray Simulation	*	
Substituent Effect <sup>a</sup>		*
Oligomer Comparison		*
Spectroscopy		
Strain Dependent Shift	*	*
Molecular Potentials	*	
Morse C-C Comparison	*	*
Simple Molecule C-C	*	*
Empirical Force Constants	*	*

<sup>a</sup> Substituents in PDA refer to the fact that while PDA has a simple carbon backbone, it is synthesized with various large chemical groups bonded to the backbone. Calculations were initially performed with hydrogen atoms bonded to the backbone to make the calculations simpler.

In this thesis I will first outline the Hartree-Fock method and the additional approximations made in the semi-empirical approaches. The ab-initio and semi-empirical methods have been exhaustively documented in the scientific literature, and the reader will be directed to appropriate references for complete treatments. An outline of the approaches is illuminating because it lays the foundation for the ultimate applicability of the semi-empirical method to the question at hand. The accuracy of the SE formulation used in this work to its calibration set of compounds will be discussed, as well as the procedure used to obtain the data from which the polymer mechanical properties is obtained. Next, a brief description of the pertinent mechanical properties and the various techniques by which they are measured will follow, as well as the calculation of these properties from the SE results. The results of the calculations on PE will be presented, as well as comparisons with experimental results. The results of the calculations on PDA will then be presented. Following this, an analysis of the results and a discussion of the implications of the results to the central question of this thesis, the appropriateness of the SE technique to the calculation of polymer mechanical properties away from equilibrium, will be presented. These comparisons provide evidence that SE calculations systematically overpredict the modulus by 20% to 25%.



## II APPROXIMATE MOLECULAR STRUCTURE CALCULATIONS

### Ab Initio Method

The Schrodinger wave equation for atomic hydrogen, the archetypal one-electron system, describes the motion of the electron in the Coulomb potential of the nucleus. The wave equation is an eigenvalue problem of the form

$$H | \Psi \rangle = E | \Psi \rangle \quad (1)$$

where  $H$  is the Hamiltonian operator. For atomic hydrogen,  $H$  is simply

$$H = -\frac{\nabla^2}{2} + \frac{1}{r} \quad (2) \text{ (Atomic Units)}$$

where  $-\frac{\nabla^2}{2}$  is the kinetic energy operator and  $\frac{1}{r}$  is the spherically symmetric Coulomb potential of the nucleus. This equation is separable in spherical polar coordinates, and the eigenfunctions are products of spherical harmonics in the angular variables  $\Theta$  and  $\phi$  and associated Laguerre polynomials in  $r$ . The wavefunctions take the form

$$\Psi_{n l m}(r, \Theta, \phi) = R_{nl}(r) \Psi_{lm}(\Theta) e^{im\phi} \quad (3).$$

The indices arise from the allowed values of the separation constants, and the different solutions describe allowed discrete states for the hydrogen electron.<sup>3</sup> The wavefunction corresponding to an allowed combination of the indices  $n, l, m$  is referred to as an orbital which the electron is said to occupy. One follows the same procedure to solve the wave equation for a system of interacting electrons and nuclei, except that separable solutions

cannot be obtained. The Hamiltonian for a system of  $n$  electrons and  $M$  nuclei is

$$H_T = \underbrace{-\sum_{i=1}^n \frac{\nabla_i^2}{2}}_I - \underbrace{\sum_{A=1}^M \frac{\nabla_A^2}{2}}_{II} - \underbrace{\sum_{i=1}^n \sum_{A=1}^M \frac{Z_A}{R_{iA}}}_{III} + \underbrace{\sum_{i=1}^n \sum_{j>i}^n \frac{1}{r_{ij}}}_{IV} + \underbrace{\sum_{A=1}^M \sum_{B>A}^M \frac{Z_A Z_B}{R_{AB}}}_{V} \quad (4)$$

- I                      II                      III                      IV                      V
- I    Kinetic energy of the electrons  
 II   Kinetic energy of the nuclei  
 III   Coulomb potential between electrons and nuclei  
 IV   Electron-electron repulsion  
 V    Nuclei-nuclei repulsion.

The wave equation for the system is

$$H_{\text{Total}} \Psi(1,2 \dots n; 1,2, \dots M) = E_{\text{Total}} \Psi(1,2 \dots n; 1,2, \dots M) \quad (5)$$

where  $\Psi$  is the wavefunction for all particles in the molecule and  $E$  is the total energy of the system. Since each particle has three degrees of freedom, this is a nonseparable partial differential equation in  $3n + 3M$  variables.<sup>4</sup>

One now applies several approximations to simplify this problem. The first is the Born-Oppenheimer approximation, which asserts that because of the large mass difference of the electrons and the nuclei, the nuclei can be considered to be fixed on the timescale of electronic motion. Thus, one

can initially neglect the kinetic energy of the nuclei and consider the nuclear repulsion a constant (which does not affect the solution of the electronic eigenvalue problem). One first solves the wave equation for the electronic Hamiltonian, which gives the electronic wavefunctions that depend explicitly on the electron coordinates but only parametrically on the nuclear coordinates. After the electronic problem has been solved, the motion of the nuclei is calculated using the average value of the Coulomb potential generated by the electrons. Solutions to the nuclear wave equation describe the vibration, rotation, and translation of the molecule.

The next step in the approximate solution of the multi-electron wave equation is to seek a form of the multi-electron wavefunction from a combination of functions which depend on the coordinates of only one electron. The simplest way to do this is to write the total wave function as a product of one electron wave functions

$$\Psi(1,2,3 \dots n) = \phi_1(1) \phi_2(2)\phi_3(3) \dots \phi_N(n) \quad (6)$$

The probability density function,  $\Psi^2$ , which describes the average location of the electrons is then a product of the one electron probabilities  $\phi_i^2$ . This description is accurate only when the events associated with each of the probabilities occur independently of each other. Thus, the physical model used in this approximation is that the electron motions are independent of each other, while in reality correlation of electronic motion is important. A multi-electron wavefunction of this form also violates the anti-symmetry requirement for the wavefunction which arises from the Pauli exclusion

principle.<sup>5</sup> A discussion of electron spin and symmetry requirements of the wave functions is omitted here; these considerations require more complex combinations of one electron wave functions to be used to represent the multi-electron wavefunction.<sup>6</sup>

Neglecting electron-electron repulsion (in addition to the nuclear terms), the multi-electron Hamiltonian could be written as a simple sum of one electron Hamiltonians. Solutions to the wave equation for each electron could be obtained analytically by separation of variables, and the exact solution to the multi-electron wavefunction would be the product of the one-electron wavefunctions. Because the inter-electron (pairwise) repulsion depends on the instantaneous coordinates of two electrons, the exact solution cannot be expressed in a separable form. However, by considering the interaction of an electron  $i$  with all the other  $n-1$  electrons as an interaction with an average, effective potential, Fock<sup>7</sup> was able to derive approximate one-electron Hamiltonians based on the earlier work of Hartree<sup>8</sup>. The Hartree-Fock equations have the form:

$$F \Psi = [H_{\text{core}} + (\sum_j (2 J_j - K_j))] \Psi_{ij} = \sum_j E_{ij} \Psi_j \quad i=1,2,3,\dots,n \quad (7)$$

Here  $F$ , the Fock operator, may be considered an effective one-electron Hamiltonian for the electron in the molecular environment, and its various terms have simple physical interpretations.  $H_{\text{core}}$  is the one-electron Hamiltonian for an electron moving in the field of bare nuclei. The term  $2J_j$ , with  $j$  not equal  $i$ , is the averaged electrostatic potential of the two electrons (of opposite spin) in the orbital  $\Psi_j$ . The exchange potential  $K_j$

arises from the indistinguishability of fermions.

In order to calculate the wavefunctions using the Hartree-Fock equations, one needs to calculate the average potential from  $n-1$  electrons in the molecule, which is determined by their locations, which is described by their wavefunctions, i.e., you need to know the answer to calculate the answer. The general process for solving the Hartree-Fock equations is an iterative process. First, one assumes a set of trial solutions,  $\Psi_1', \Psi_2', \dots, \Psi_n'$  which allows computation of the coulomb and exchange operators and thus a first approximation to the Fock operator. The eigenfunctions of this operator are used as a second approximation to the wavefunctions, and the procedure is repeated until the Fock operator no longer changes (to a given tolerance). These wavefunctions are said to be self consistent with the potential field they generate, so this procedure is known as the self-consistent field (SCF) method.

The choice of the trial wavefunctions is important to the solution. The most commonly used choice is to approximate the Hartree-Fock wavefunctions with linear combinations of atomic orbitals (LCAO). Since the atomic orbitals (Eqn 3) are orthonormal functions, this is a finite generalized Fourier series expansion of the molecular orbitals. This selection has the further advantage in aiding the interpretation of the results since the molecular properties can now be related to those of the constituent atoms. The atomic orbitals used to construct the molecular orbitals are called a basis set. Better representations of the molecular

orbitals can be obtained by including more terms in the expansion, a larger basis set, though this increases the computation time. In practice, the atomic orbitals themselves are approximated by a series expansion because the actual atomic wavefunctions are computationally difficult to evaluate. A common choice is to use Gaussian functions; strictly speaking this is not a proper choice because Gaussians are not orthogonal functions; however, the basis set can be orthogonalized with an additional operator.

When you start adding up all the terms in the molecular orbitals it becomes apparent why ab-initio Hartree-Fock calculations become complex very quickly. For example, consider the diatomic molecule HF. One needs six atomic orbitals to represent each molecular orbital. If one uses 6 Gaussian functions to represent each atomic orbital, one would have  $36 \times 36 \times 6$  complicated integrations to perform on each iteration of the SCF procedure. In practice, many of these integrals do not need to be recalculated on each iteration, and can be stored on disk; however, a high level calculation on a fairly simple system can easily consume gigabytes of disk space. There are many other considerations that make the ab-initio implementation of the Hartree-Fock method computationally expensive, both in terms of CPU time and disk space, which are omitted from this discussion for the sake of brevity. The net result is that while ab-initio calculations give very good results (when compared to experiment), the computational cost is prohibitive for all but fairly small molecules.

It should be noted that because the Hartree-Fock method explicitly neglects electron correlation, the result of a Hartree-Fock calculation, even

with a basis set of infinite size, will always be higher than the true minimum of the system. Inclusion of electron correlation tends to decrease the calculated bond stiffness, which implies that even ab-initio Hartree-Fock calculations of mechanical properties may be systematically high.<sup>9,10</sup> A complete discussion of the theory of ab-initio Hartree-Fock method is found in Szabo and Ostlund.<sup>6</sup>

### Semi-Empirical Method

In order to enable the calculation of larger molecules, additional approximations are required than those used in the ab-initio method. The most difficult and time consuming procedure of the ab-initio method is the computation of the large number of two electron (repulsion or exchange) integrals. One can argue from physical considerations that many of these integrals should be very small, a fact which can be verified by doing the calculation. One important class of electron-electron interactions that is small is the overlap between different atomic orbitals describing the molecular orbital of an electron, e.g., the overlap between a 1S and 2P orbitals from the same atom is essentially zero. The overlap between two different atomic orbitals describing the molecular orbital of an electron is referred to as differential overlap (DO). If the atomic orbitals originate from the same atom, it is called monatomic differential overlap: if from different atoms it is called diatomic differential overlap. By assuming differential overlap to be negligible, a large number of integrals involved in the Fock operator can be set to zero (Neglect of Differential Overlap). This

assumption formed the basis for the first semi-empirical method, the complete neglect of differential overlap (CNDO) method introduced by Pople, Santry, and Segal<sup>11</sup>. In addition to NDO, only valence electrons are treated explicitly, while inner shell electrons are treated as part of the nuclear core, modifying the nuclear potential in the core Hamiltonian ( $H^{\text{core}}$ ). Additional based semi-empirical methods include intermediate neglect of DO (INDO), modified intermediate neglect of DO (MINDO), modified neglect of DO (MNDO), etc. <sup>11</sup>

Another essential simplification in the SE method is the treatment of interaction integrals in the Hamiltonian as element specific parameters . The number of parameters required to describe an element corresponds to the number of interaction terms in the approximate Hamiltonian used. Examples of parameters would be the one-electron energy of an atomic orbital of an ion (bare nucleus + core electrons) resulting from the removal of all valence electrons, an atomic Slater orbital exponent, or the exponent in a gaussian describing core-core repulsion. The name semi-empirical arises because some of these parameters are obtained from experimental data.

Within the SE approach, the self-consistent field algorithm is used to calculate the molecular orbitals while the calculation of a large number of complicated integrals in the ab-initio method is replaced by a relatively small lookup table. Thus a semi-empirical calculation is simplified, as is shown in Fig 1, by a comparison of the ab-initio (1a) and SE (1b) approaches which is reproduced from Clark<sup>12</sup>. The combination of greatly reduced



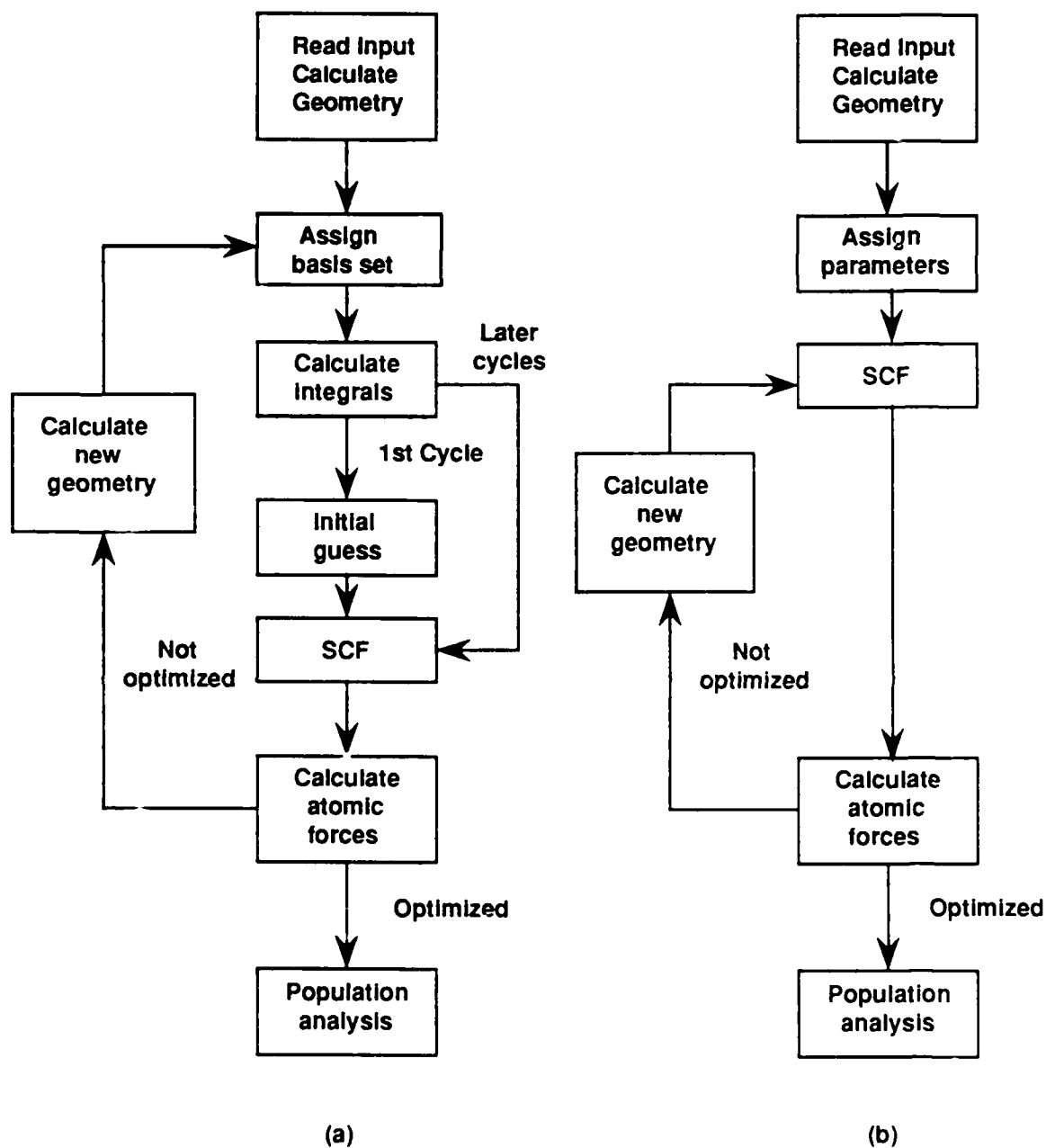


**Figure 1.** Typical flow charts for (a) an ab-initio optimization and (b) a corresponding semi-empirical calculation.

computation times and memory requirements means that much larger systems can be treated by SE methods than by ab-initio techniques. Moreover, the accuracy of the SE methods in calculating heats of formation compares favorably on a wide range of systems when compared to moderate level ab-initio calculations. Note, however, that this is not true for all molecular properties.<sup>13</sup>

The ultimate success of a semi-empirical method hinges on the validity of the approximate Hamiltonian used and on the values of the parameters used. Ideally, one would want the parameters that describe each element to be completely independent of the molecular environment, i.e. the parameters which describe a carbon atom in  $\text{CH}_4$  should give results of the same accuracy when used in  $\text{CF}_4$ . In reality, the specific molecular environment does affect the atomic parameters. In order to make the application of the method generic the parameters are selected to minimize the least squares error for selected molecular properties over a large set of molecules.

It should be noted that the use of experimental data to define some of the parameters actually gives the semi-empirical method some advantage over the ab-initio method. The measured quantities inherently contain all the physics involved and so are not limited by the approximations used to define a tractable Hamiltonian. A complete discussion of SE methods is presented by Pople and Beveridge.<sup>4</sup>

The Austin Model 1 (AM1) semi-empirical Hamiltonian (and

parameters) were used in the calculations in this thesis. AM1 is an extension of the earlier MNDO/3 Hamiltonian which is known to overestimate nuclear core-core repulsion. Thus the parameters for the AM1 include those from the approximate Hamiltonian as well as Gaussian exponents describing the modified core-core repulsion. Five of the parameters were assigned values from atomic spectroscopy. The other parameters were initially estimated and adjusted to best reproduce the following experimental equilibrium (297 K) gas phase properties:

1. Heat of Formation
2. Dipole Moments
3. Ionization Potentials
4. Molecular Geometries.

Most of these properties used in the parameterization are obtained from experiment, though for some molecules on which precise measurements are impractical, the results of high level ab-initio calculations are considered reliable enough to be used. Table 2, which reproduces Table XII from Stewart <sup>14</sup> shows the average error in the calculation of molecular geometries associated with the AM1 method. A detailed statistical analysis of the errors associated with AM1 with respect to these four properties is presented in ref 11. Of these benchmark properties only comparisons with equilibrium molecular geometry will be performed in this study.

TABLE 2

## AVERAGE ERRORS IN MOLECULAR GEOMETRIES

Geometric Parameter	Number of Molecules for Comparison	MNDO	AM1	PM3*
Bond Length [Å]	372	0.054	0.050	0.036
Bond Angle [Deg]	158	4.342	3.281	3.932
Torsion Angle [Deg]	16	21.619	12.494	14.875

\*The PM3 Hamiltonian is a modification of MNDO which gives better results for hypervalent compounds.

## Semi-Empirical Calculations of the Electronic Structure of Polymers

While large molecules can be handled by the semi-empirical method, an ideal polymer is an infinite chain molecule; clearly an approximation must be made to calculate polymer properties, even within the SE approximation. One technique is to consider a series of small molecules which are made up of increasing numbers of the polymer repeat units, namely oligomers. The oligomer properties will not accurately represent the polymer properties, but one can extrapolate the results as a function of repeat units to the infinite repeat unit result. Drawbacks to this method are that it is time consuming and end effects will always be present in the oligomers which are not found in polymers. Another approach is the cluster method developed by Perkins and Stewart.<sup>15</sup> In the cluster method, one performs calculation on a cluster, which is a number of polymer repeat units. The atom at one end of the cluster interacts with the atom at the

other end, as though it were connected in a ring. Ref 15 provides a good discussion of how this approach for a cluster of carbon atoms reduces to Huckel theory for benzene. Using the cluster, exact results for an infinite molecule can be reproduced with as few as one repeat unit, provided the repeat unit is long enough to make an acceptable cluster. The number of repeat units required in the cluster is driven by the electron de-localization length in the polymer; the length of the cluster must be large enough so that any one atom does not interact with itself through the cyclic boundary conditions. Stewart suggests that a cluster length of 10 Å is sufficient for most polymers, except those containing conjugated Pi bonds, where a cluster length of 20 Å is recommended. This was verified in this study for PDA, where the heats of formation and repeat unit lengths were monitored as a function of cluster size. PE has been previously calculated using the cluster method with the MNDO/3 Hamiltonian, so that the cluster length dependence is known. <sup>1</sup>

#### Details of the Calculations

The program MOPAC version 5.0 was used with the AM1 Hamiltonian was used in this study with the unrestricted Hartee-Fock (UHF) method. <sup>16</sup> The cluster method as described in ref 15 was used to simulate ideal polymer chains. Strain dependent geometry optimizations were performed by using the translation vector, which describes the length of the cluster and defines the polymer connectivity, as a reaction coordinate for a series of strain values. All MOPAC calculations were performed on a Silicon Graphics workstation in the Polymer Branch of the Materials Laboratory at

WPAFB. Ab-initio oligomer calculations were performed using the programs GAUSSIAN88 and GAUSSIAN90<sup>17</sup> on Elxsi and Cray supercomputers.

### III RELATIONSHIP OF THEORY TO EXPERIMENT

#### Calculations of Mechanical Properties

The basic method used to determine the mechanical properties of a polymer is to measure the amount of force required to change the length of a sample. From this measurement one obtains a stress (force per unit area) strain (fractional change in length away from equilibrium) curve. A generic stress-strain curve is shown in Fig 2. Several mechanical properties, defined by the behavior of the stress-strain curve, are labelled. The modulus is the initial slope of the stress-strain curve. The yield strength is the amount of force at the point where the slope of the stress-strain goes to zero, i.e., the resistance to deformation vanishes. The ultimate strength is the force at the point where the material physically breaks. If one had a perfectly ordered, perfectly aligned, defect-free crystalline polymer, the stress-strain curve measured on the bulk material would be identical to the properties of a single polymer chain.

Straining a molecular system, i.e., increasing or decreasing the separation between the atoms, requires energy, so that the potential energy of the system increases when it is constrained to a non-equilibrium length. To a first approximation, the interaction between two atoms in a molecule can be described as a harmonic oscillator (ideal spring). For an ideal harmonic oscillator (H.O.), this energy is proportional to the square of the deviation from the equilibrium separation. The force required to stretch (or squeeze) a spring is proportional to the second derivative of the potential energy curve with respect to position. The second derivative of a quadratic

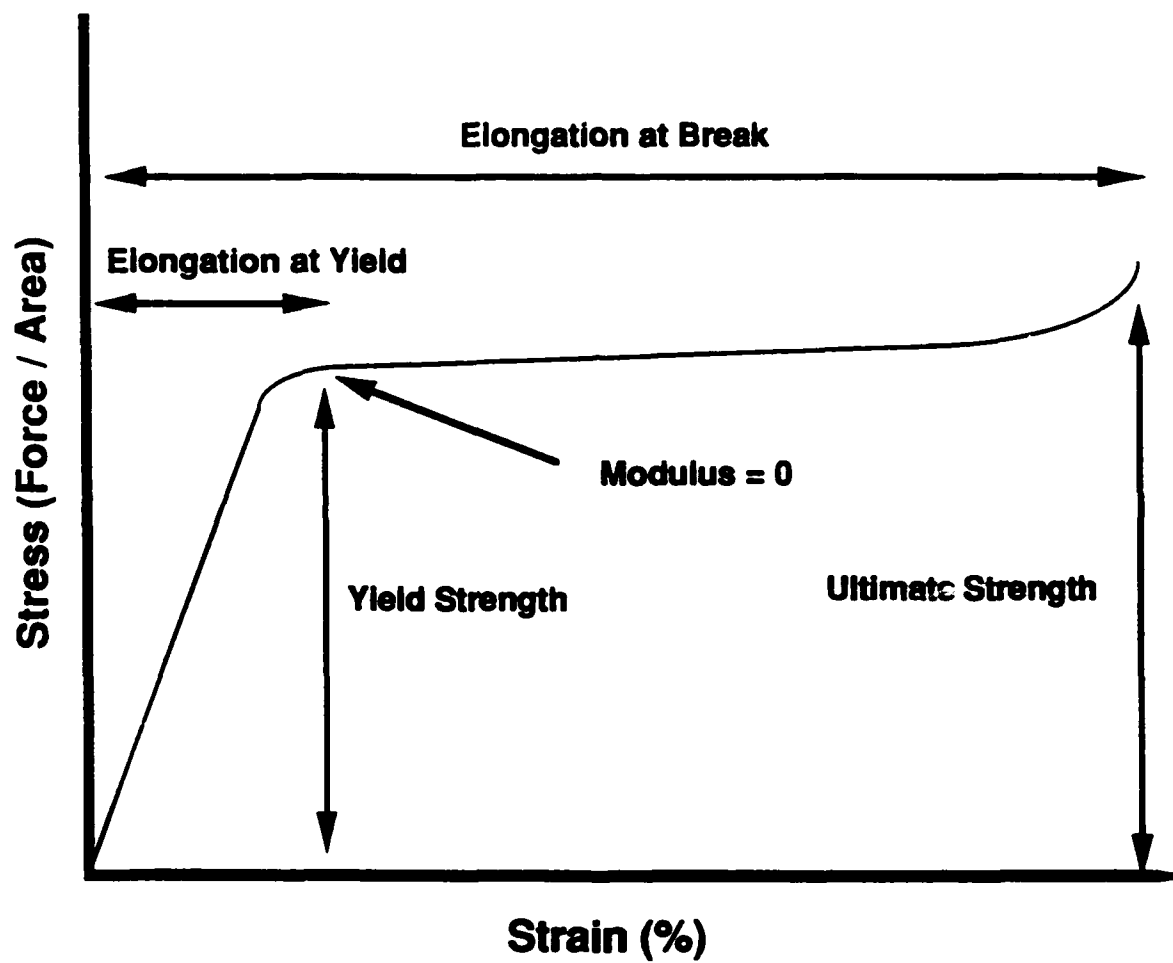


**Figure 2. Generalized tensile stress-strain curve for a polymer**



potential is a constant, so the stiffness of a spring is described by a force constant. The resistance of a material to deformation is described in terms of its modulus, the force per unit area required to distort it from its equilibrium length (along a specific axis), which is equal to the initial slope of the materials' stress-strain curve. The modulus of a spring then is the second derivative of its energy potential (force constant) times its equilibrium length divided by its cross sectional area.

The energy potential curve of a strained molecular system can be generated through semi-empirical calculations. First, one determines the equilibrium geometry of the molecule by optimizing all its variables (bond lengths, bond angles, torsion angles). Associated with this optimum equilibrium geometry is a heat of formation. One then changes a variable which describes the overall molecular length, e.g. increase the length by 2%, and then calculates the optimum geometry for the molecule with this variable fixed. Clearly, the heat of formation for this strained geometry will be higher than equilibrium. By calculating the heats of formation for a number of such strain values one can map out the potential energy curve for the molecule. The second derivative of this curve is the spring constant of the molecule, which can be used to calculate its modulus (on a molecular level, the crystal unit cell area is used for the cross sectional area). For a polymer, one fixes the length of the cluster, optimizes the geometry of the repeat unit and obtains the minimum energy for a particular strain. For a polymer, this energy is an amalgam of all the various deformation modes (bond extensions, bond angle changes, and torsion angle twists).

Comparing the calculated cluster modulus with experiment is not a sufficient test of the validity of the calculation because compensating errors in the calculated deformation modes could combine to produce a value for the modulus which seems "reasonable", i.e., is less than several orders of magnitude larger than experiment.

There is a potential problem inherent with this technique: the parameters used in AM1 were optimized to reproduce the equilibrium heat of formation. There is no guarantee that the heats of formation are meaningful away from equilibrium. One may have an accurate value of the potential at equilibrium, but the optimization procedure includes information about the quality of the energy derivatives. Because the mechanical properties of a material depend on the derivatives of the potential, in order to assess the accuracy of the calculation of a material's mechanical properties, one must investigate the accuracy of the potentials (and their derivatives) used to describe the molecular bonding in the material.

A more precise description of a molecular bond is that only for small deviations about the equilibrium length, the potential is harmonic with displacement. At larger displacements the true anharmonicity of the potential can be observed. In general, the potential is softer than harmonic in tension (positive strain) and harder in compression (negative strain). Thus the spring "constant" for a real bond is not a constant. Common attempts to represent the anharmonicity in a real bond potential are to include cubic or higher polynomial terms. A very good, generic fit to bond

potentials is given by the Morse potential, which was originally derived as an empirical fit to diatomic spectra. The form of the Morse potential is<sup>18</sup>

$$V(r) = D_0 (1 - e^{-a(r-r_0)})^2 \quad (8)$$

where  $D_0$  is the dissociation energy of the bond,  $r_0$  is the equilibrium length, and  $a$  describes the curvature of the potential. A comparison of a Morse and harmonic potentials is shown in Fig 3.

The vibrational frequency of a diatomic molecule is given by

$$\nu = \frac{1}{2\pi} \sqrt{\frac{k}{\mu}} \quad (9)$$

where  $k$  is the force constant and  $\mu$  is the reduced mass of the two atoms.

For a harmonic potential, the value of  $k$  does not change so the frequency does not change with inter-atomic separation. For a system described by an anharmonic potential, the frequency changes with strain because the second derivative of the potential is no longer constant. By measuring the vibrational spectrum of a molecule one obtains the value of the second derivative of the potential at equilibrium. Measuring the shift of the vibrational frequencies with strain provides information about the anharmonicity of the potential. Thus by comparing measured vibrational shifts with those calculated by AM1 it is possible to determine the accuracy of the calculated bond stiffness.

One can directly calculate the strain dependent potential of a single bond in a molecule by constraining just that particular bond length and optimizing the rest of the geometry. This proved to be very useful for

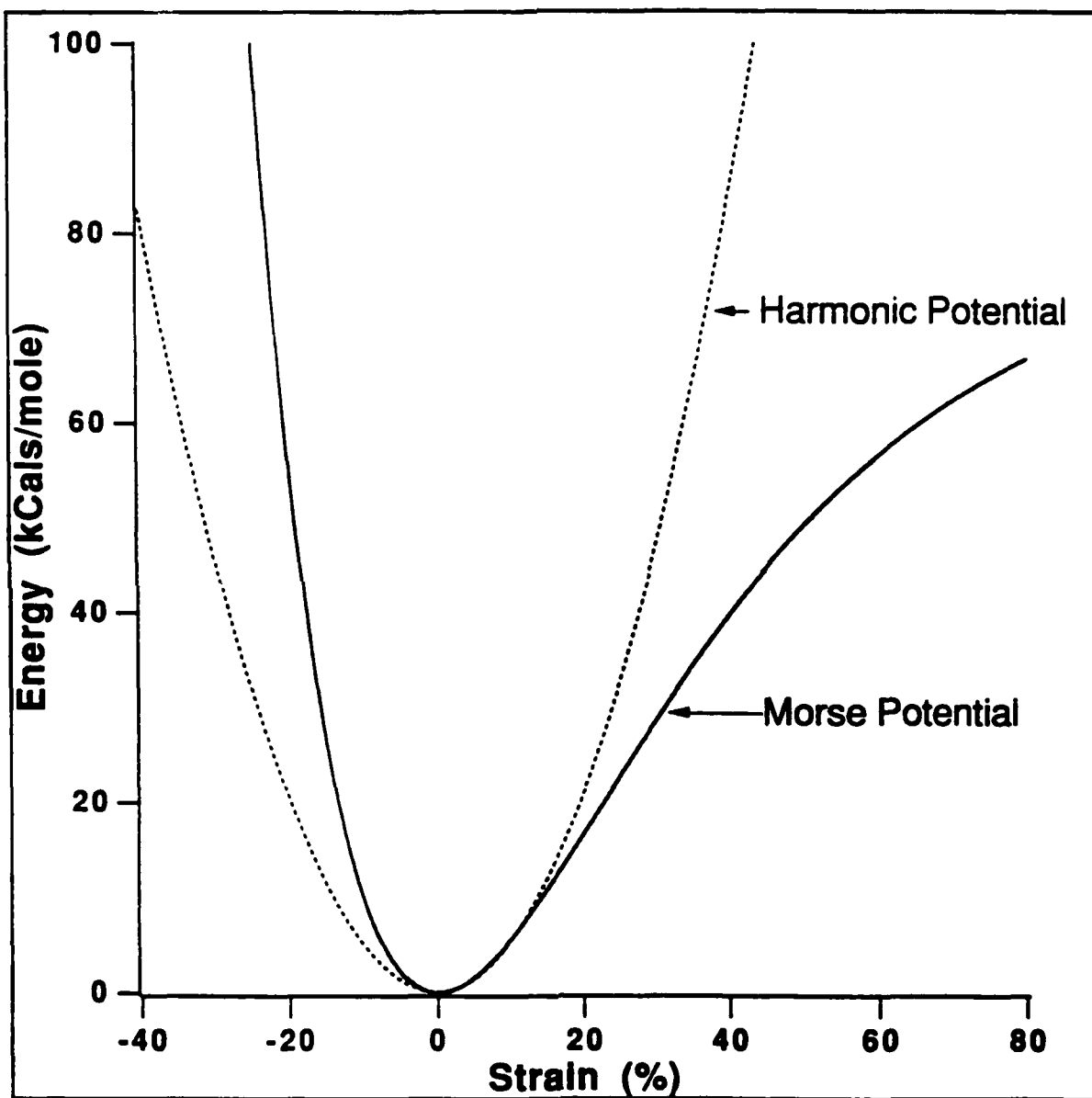


**Figure 3.** Comparison of Morse and harmonic potentials. Both have the same second derivative at equilibrium.

polyethylene because Wool<sup>19</sup> provided a Morse potential for the C-C bond stretch which was used to calculate the modulus. This Morse potential is judged to be a good representation of the C-C bond because it matched both the absolute frequencies and the strain dependent frequency shifts observed in polyethylene.

It is known that the calculation of vibrational frequencies from the SE (or an ab-initio) method produces results which systematically overestimate the measured frequencies.<sup>6</sup> This discrepancy is a result of the method used to calculate the frequency rather than inherent in the SE method itself. The force constant is calculated by taking the second derivative of the potential at equilibrium. The vibrational energy levels of a harmonic oscillator are

$$E(v) = -D_0 + \frac{h}{2\pi} \omega \left(v + \frac{1}{2}\right) \quad (9)$$

where  $D_0$  is the minimum of the potential,  $v$  is a non-negative integer, and

$$\omega = \sqrt{\frac{1}{\mu} \frac{d^2V(r)}{dr^2} \bigg|_{r=r_0}} \quad (10)$$

In equation (10),  $\mu$  is the reduced mass of the molecule. The vibrational energy levels of a Morse potential are

$$E(v) = -D_0 + \frac{h}{2\pi} \omega \left\{ \left(v + \frac{1}{2}\right) - \frac{1}{\zeta} \left(v + \frac{1}{2}\right)^2 \right\} \quad (11)$$

$\zeta$  is defined such that the anharmonic  $\left(v + \frac{1}{2}\right)^2$  term can never exceed the harmonic  $\left(v + \frac{1}{2}\right)$  term.<sup>20</sup> It is seen by a comparison of Eqns (9) and (11) that the energies of the harmonic and Morse potentials will differ

significantly only if  $\nu$  is large. This is not the case for the  $\nu=1$  state as calculated by the SE codes, or if the energy separation between the minimum of the potential and the  $\nu=1$  state is large, which occurs if  $\mu$  is small. This approximation in the frequency calculation, as well as the neglect of electron correlation, produces systematic errors; because comparisons are made to strain dependent frequency differences, the systematic error cancels out and comparisons with experimental strain dependent frequency shifts is meaningful.

Matching vibrational frequencies and shifts is more complicated for polyatomic molecules than diatomics because the normal modes of vibration involve displacement of several atoms simultaneously (and because the number of vibrational frequencies scales as  $3n-6$ ), hence it is more difficult to isolate the individual bond force constants involved. Although an ideal polymer has an infinite number of atoms, its repetitive structure results in many degenerate vibrational modes, and so interpretation of the spectra is tractable.

#### Measurement of Polymer Modulus

As stated before, the measurement of the bulk mechanical properties for a polymer by obtaining its stress-strain curve does not represent the ultimate mechanical properties for that polymer. Fig 4 shows the structure of a typical amorphous polymer, in which the polymer chains are randomly oriented and twisted around each other. When one strains a bulk

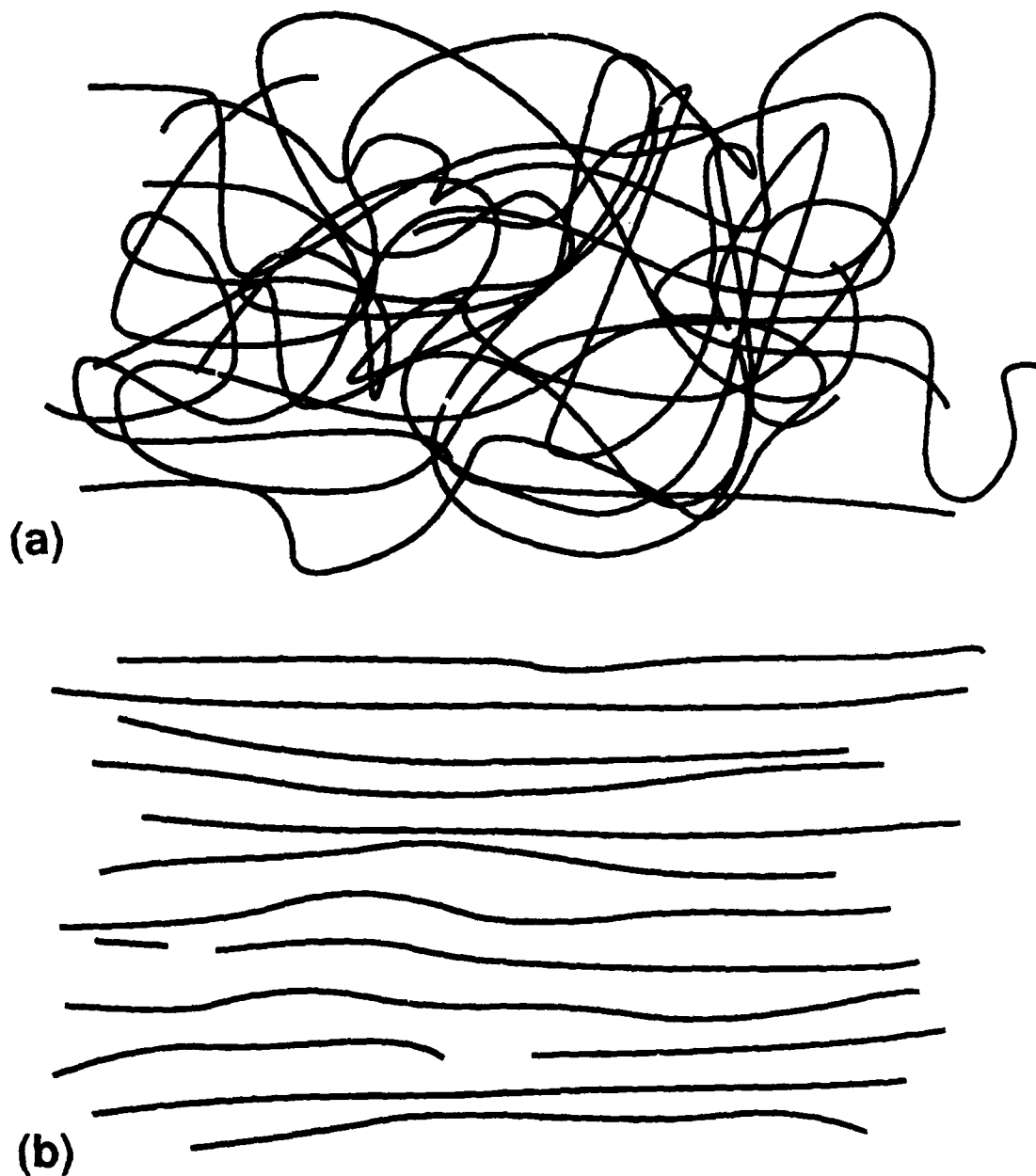


**Figure 4.** Amorphous polymer structure (a) and idealized structure (b). In the ideal structure, all the chains are oriented along the same axis; the only limit to bulk stiffness other than chain stiffness is the presence of chains which do not extend the full length of the sample (chain ends).

sample of an amorphous polymer, one is addressing primarily the strengths of the inter-chain interactions. Only those regions whose chain axis is aligned with the axis of strain will resist with the chain strength. As the degree of order is increased in the polymer, by better aligning the chain along one axis, the mechanical modulus of the polymer will increase. If the individual chains were perfectly aligned, the mechanical modulus would equal the ultimate axial modulus (the transverse modulus, however, would be minimized). In practice, "perfect" alignment can only be obtained in a limited number of polymers, of which PDA is one which can be polymerized in single crystal form. Mechanical properties in PDA are not constrained by alignment but by crystal defects, chain ends and other chemical imperfections.<sup>21,22</sup>

The calculations of polymer moduli are performed on an ideal, infinite single polymer chain, which simulates perfect polymer morphology and neglects the role of interchain forces. While this scenario is unrealizable in a practical sense, it is useful because it defines the upper bound for the mechanical properties of a given polymer. Comparisons of this upper limit for different polymers is useful because if the degree of alignment one can obtain in processing is roughly equal for all polymers (or at least a class of chemically similar polymers), the polymer with the stiffest /strongest chain will make the stiffest/strongest bulk material. An analysis of the deformation modes can also give insight into what chemical structures contribute most to mechanical strength and stiffness.

Since mechanical measurement does not represent the ultimate limits



of a polymer, other techniques are employed to make molecular level measurements. X-ray diffraction is used to monitor the location of the  $2\theta$  peak which corresponds to the chain length; in PE this is the (002) peak. (In this study, the polymer axis will be defined as the  $c$  crystal axis.) A calibrated force is applied to the polymer to elongate it, and the strain of the  $c$ -axis is monitored from the appropriate diffraction peak. Under the assumption that stress is uniformly distributed throughout the sample (which is not always a very good assumption) one obtains a molecular stress-strain curve, whose slope is the modulus. Since this technique monitors molecular strain rather than bulk strain, the modulus measured better represents the ultimate modulus of the polymer.<sup>23</sup> Bulk PE does not have a pure crystalline structure, so X-ray modulus measurements on PE are very sensitive to the degree of crystallinity. The X-ray modulus of PDA should equal the ultimate theoretical modulus because it can be polymerized in single crystal, though defects may play a role in the measurement. The X-ray modulus of PDA has not been reported to date.

Another method of measuring the ultimate moduli of polymers is to derive the force constants associated with the bonds from the polymer's spectra and calculate the effective axial deformation force constant from them. This technique is difficult to apply in practice because it is difficult to perform the normal vibrational mode analysis on the polymer and deconvolve the individual force constants from the complex spectra. While this method has no predictive capability on proposed polymers, in theory a

force constant analysis should give the correct value for the modulus because it is based on measured force constants, i.e., there are no approximations made to obtain the result. In practice, for all but simple polymers the mode structure is so complex that researchers often used measured values as a first guess, and then adjusted the force constants to fit the spectra. The set of force constants obtained in the fitting in many cases is not unique, and so the advantage of being based on measurement is lost.

This discussion of mechanical properties is intended to be a generic description. The mechanical behavior of polymers is much more complicated, and differs greatly from polymer to polymer for very material specific reasons. A good introduction to the mechanical behavior of polymers is presented by Young.<sup>20</sup>

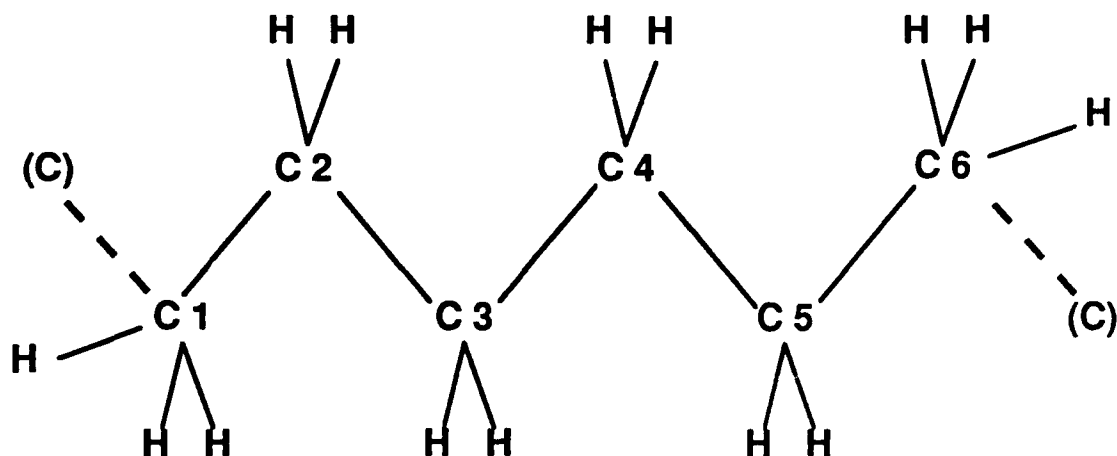
## IV POLYETHYLENE RESULTS AND DISCUSSION

### Molecular Structure and Modulus Calculations

Polyethylene (PE) chains are comprised of single carbon-carbon bonds in a planar zigzag structure, which is one of the simplest structures possible for any polymer. Comparisons between the molecular structure results obtained by the SE and ab-initio methods were performed on the PE oligomer shown in Fig 5. The cluster used in the SE polymer calculations is identical to the oligomer shown except that there are only two hydrogens bonded to C1 and C6, the periodic boundary conditions establishing a carbon-carbon bond at the appropriate distance and angle between C1 and C6. The SE carbon-carbon bond distances are approximately 0.04 angstroms shorter than the ab-initio distances. The C-C bond distance in PE, obtained from X-ray diffraction, is 1.53 Å.<sup>24</sup> The SE bond angles are approximately 2 degrees smaller than the ab-initio results. The SE values for bond lengths and angles are accurate to within the published uncertainty of the AM1 Hamiltonian listed in Table 2.

In both the SE and ab-initio oligomer results, bond lengths and angles are seen to depend on the location in the molecule, with the bond lengths at the end of the oligomer showing the largest variation (end effects). In contrast, the SE results with periodic conditions are essentially equal throughout the cluster, as anticipated for an ideal polymer chain.

The strain dependent heat of formation potential curve for PE is shown in Fig 6 from -10% to +10% strain. This plot is offset by the equilibrium heat of formation of the cluster, -38.9105 kCals/mole. The cluster's



Bond Length [Å]	Oligomer (C <sub>6</sub> H <sub>14</sub> )		AM1 Cluster (C <sub>6</sub> H <sub>12</sub> )
	AM1	Ab-Initio*	
C1-C2	1.507	1.559	1.513
C2-C3	1.514	1.545	1.513
C3-C4	1.513	1.544	1.513
C4-C5	1.514	1.545	1.513
C5-C6	1.507	1.559	1.513

Bond Angle [Deg]	Oligomer (C <sub>6</sub> H <sub>14</sub> )		AM1 Cluster (C <sub>6</sub> H <sub>12</sub> )
	AM1	Ab-Initio*	
C1-C2-C3	111.544	112.834	111.078
C2-C3-C4	111.365	113.565	111.110
C3-C4-C5	111.364	113.565	111.119
C4-C5-C6	111.544	112.832	111.077

\* Calculation performed at UMP2/6-31G

Hydrogen bond angles on terminal carbons not true to scale for the oligomer

**Figure 5 .** Comparison of PE oligomer and cluster geometry calculated by AM1 and ab-initio methods.

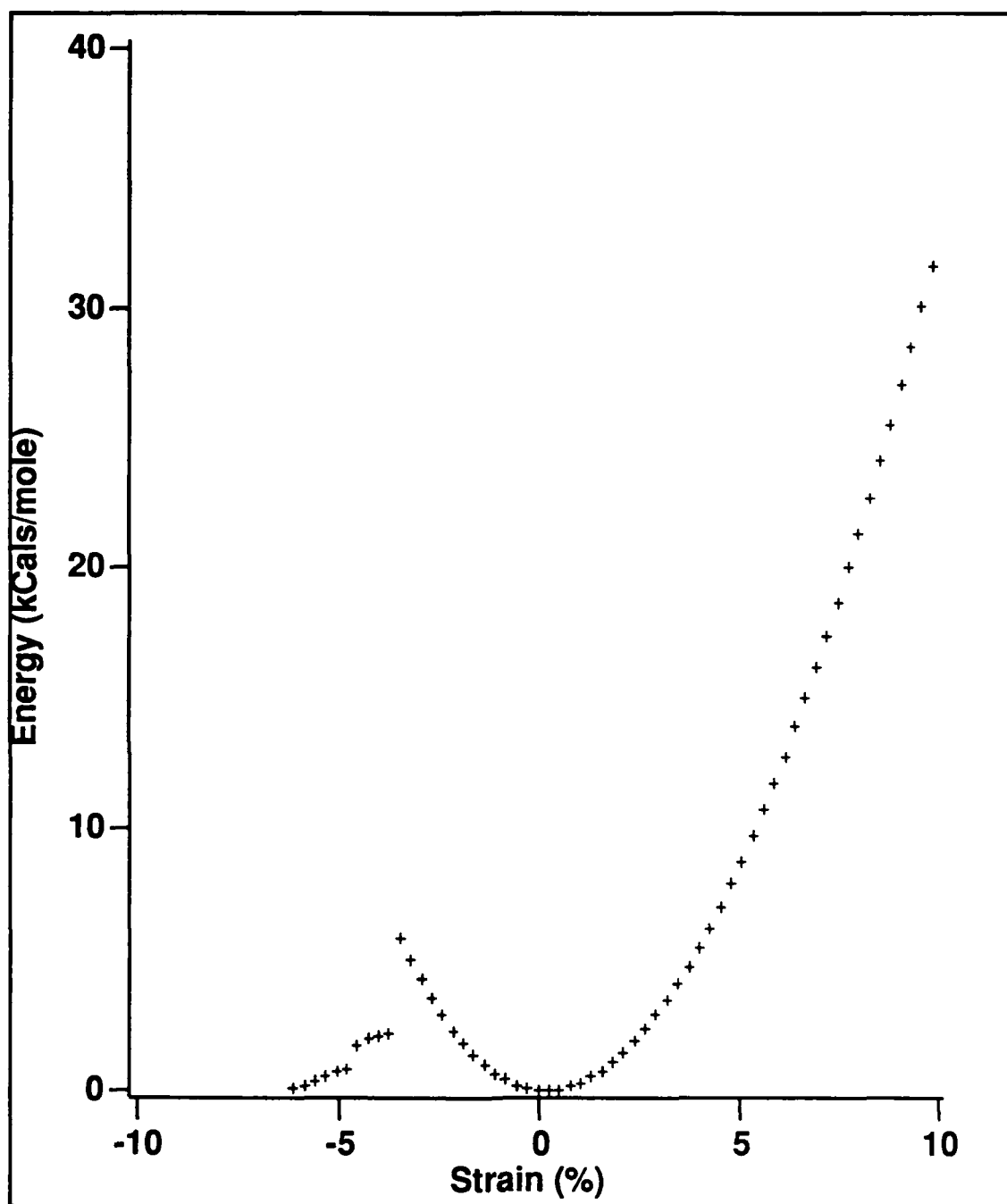


**Figure 6.** PE cluster strain dependent heat of formation. The discontinuity in the curve occurs when the cluster bends out of its equilibrium planar geometry.

equilibrium length is 7.488 Å. The discontinuity in the curve in compression occurs when PE deviates from a planar structure, i.e., the PE chain bends. This deformation mode does not directly correlate to a bulk failure mode in the polymer, however, it indicates that PE does not possess a large, inherent compressive strength<sup>25</sup>. The PE chain has not failed in tension up to 10% strain; again this does not correlate to a bulk polymer property. Since PE has a planar chain structure in the calculation, the only tensile failure mode accessible in the calculation is bond breaking. This calculation predicts that a PE chain will not fail at a uniformly distributed tensile strain of 10%.

The second derivative of the strain-dependent heat of formation curve is the restoring force of the cluster. This can be obtained several ways. One can perform a polynomial fit to the potential; then twice the second order coefficient is the force constant at equilibrium (k). The chain modulus can then be defined by

$$\epsilon = \frac{k \times L}{A} \quad (10)$$

where L is the cluster length and A the cross sectional area. In this study, the cross sectional area, obtained from the crystal structure, was taken to remain constant (18.4 Å<sup>2</sup> <sup>24</sup>) as a function of strain (Poisson ratio of 0.0). Klei and Stewart used a third order polynomial, which is the first order anharmonic perturbation to a harmonic potential, to fit the potential. The second derivative of a third order polynomial is a line, thus a cubic fit predicts that the restoring force drops off linearly with strain. One can take

the second derivative of the potential numerically and attempt to obtain the exact strain dependent behavior of the modulus predicted by the calculation. While the potential (Fig 6) appears smooth, random variations in the heat of formation values requires that smoothing be used in conjunction with the numerical differentiation. Typically, the first derivative of the potential, the force curve, is obtained directly. The force curve is smoothed with a fifth order Gaussian filter before the second derivative is taken. The second derivative curve is also smoothed. A comparison of the numerical second derivative and the second derivative from a cubic polynomial fit is shown in Fig 7. The units of the second derivative have been converted to SI, newtons per meter (Nt/m), in this figure. As is seen, both procedures agree very closely at equilibrium, with a value of  $100 \pm 5$  Nt/m.

The modulus of PE predicted by this AM1 calculation is  $400 \pm 20$  GPa. Reference 1, which used the MNDO semi-empirical Hamiltonian, predicted a value of 360 GPa. This difference is consistent with the difference in the heats of formation obtained with these different Hamiltonians. An earlier, low level ab-initio calculation of PE chain modulus reported a value of approximately 400 GPa.<sup>26</sup> The reported value for PE chain modulus, calculated and measured by the techniques discussed previously, varies from 180 to 400 GPa.<sup>27</sup> The commonly accepted value of PE chain modulus is around 300 GPa. While the AM1 value of 400 GPa is high, it is not outside the range of previously reported values. However, a priori there is no justification to claim that the AM1 result is

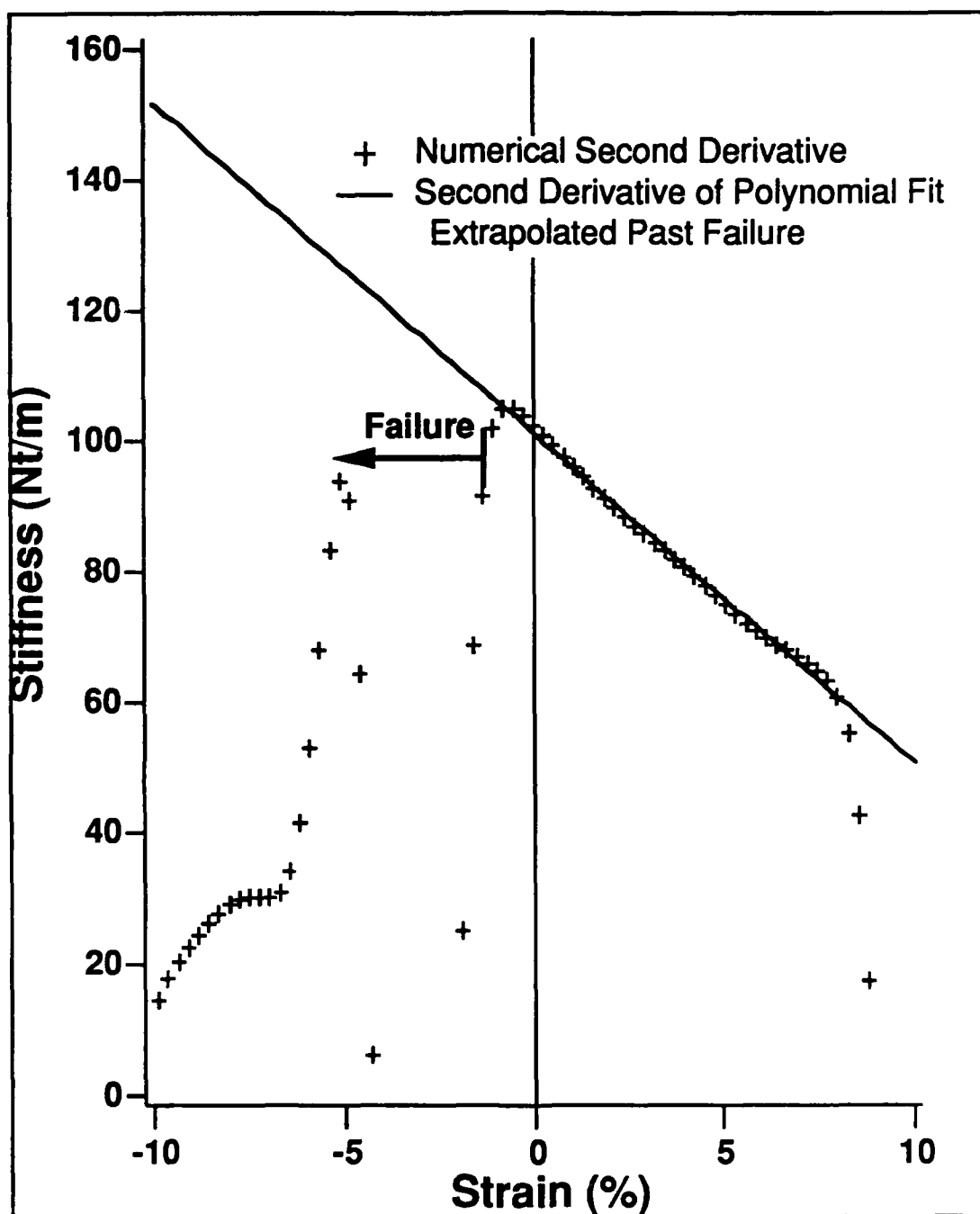


**Figure 7** Comparison of second derivatives of PE heat of formation potential. The discontinuity in the numerical derivative results from molecular failure.



more or less accurate than any of the others.

In order to investigate the accuracy of the calculation, an obvious question is to inspect the strain dependent minimum energy geometries and how the *c*-axis strain of the cluster is distributed among the various components. The length of the cluster can increase by increasing the bond lengths and bond angle; one would expect to observe the length of the cluster increase by some combination proportional to the resistance of each deformation mode. (The discussion here is limited to tension because the experiments on PE used for comparison did not report any results in compression.) A commonly used rule of thumb puts a ratio of 100:10:1 in terms of the amount of force required to change a bond length, bond angle, and torsion angle respectively.<sup>21</sup> One would then expect polyethylene to deform primarily by changing the bond angles, with a smaller contribution coming from increasing the bond lengths. (Since the equilibrium structure of PE is planar, a change in the torsion angle is considered a failure mode.)

Figure 8 shows the relative variation of the bond angles and bond lengths in PE under tension as a function of cluster *c*-axis strain. The bond angle variation is seen to be larger than the bond length variation, but not by a factor of 10. The average angular contribution to *c*-axis strain is obtained by performing a linear fit to this data, is  $0.51 \pm 0.05$ , while the bond length contribution is  $0.46 \pm 0.05$ . This shows that the *c*-axis deformation is roughly equally distributed between these two modes, not a 10 to 1 partitioning. This behavior was also reported by Wool<sup>17</sup>, and is consistent with observed spectral line shifts.

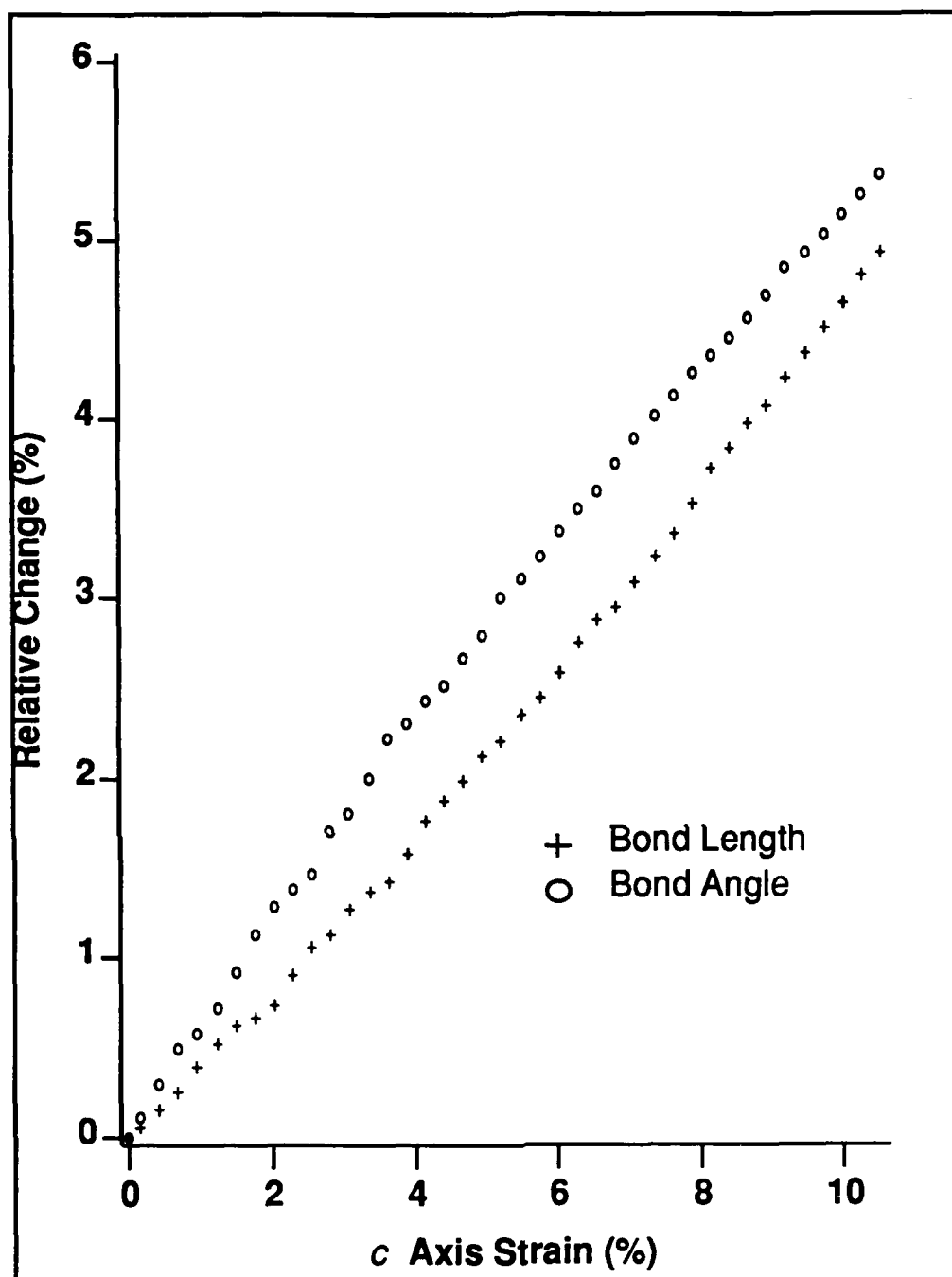


**Figure 8.** PE distribution of chain strain between bond angle and bond length.

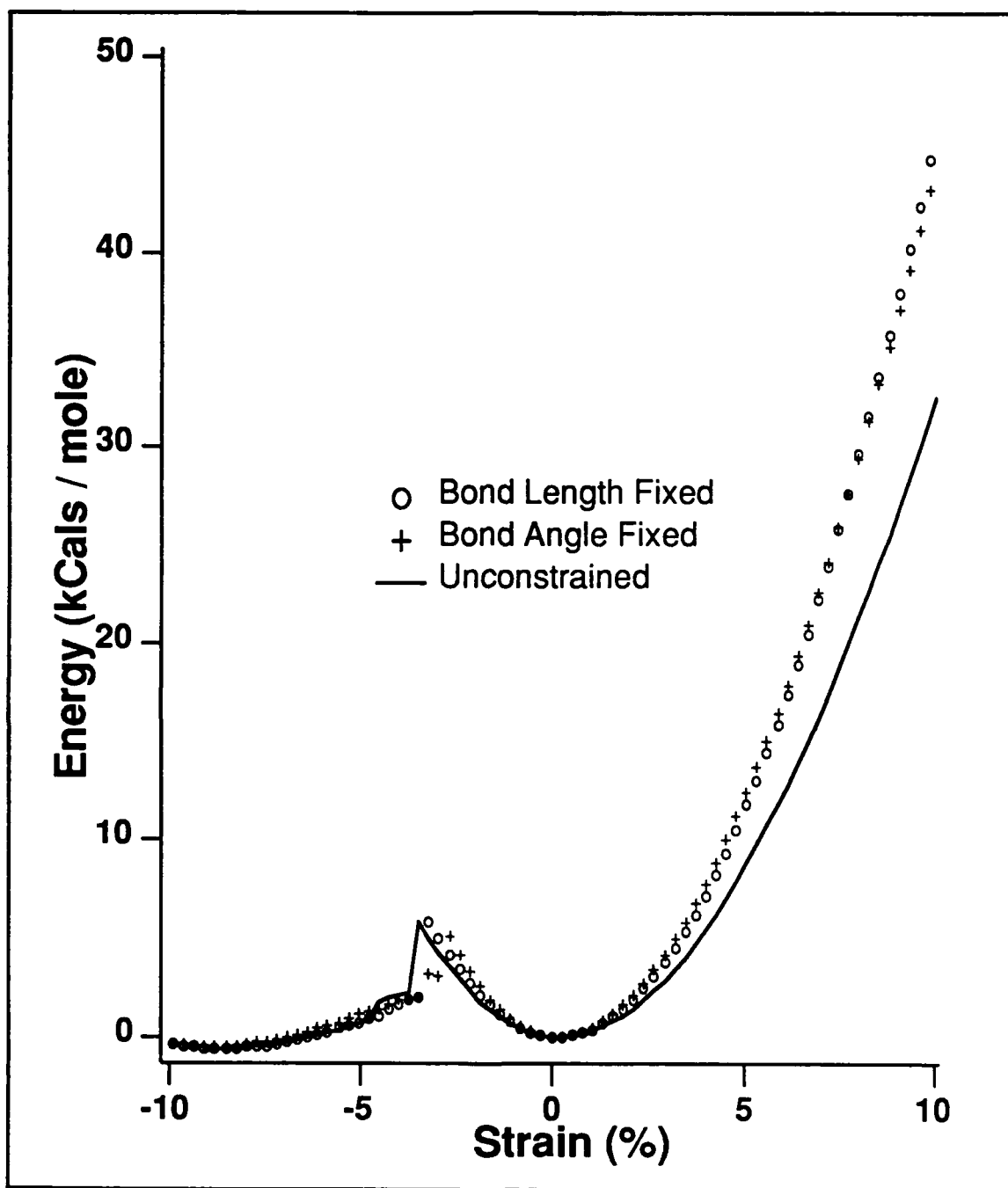


Figure 9. PE cluster strain potentials with bond angle and bond length fixed. The unconstrained potential, i.e., nothing fixed, is shown for comparison.

As a check on this behavior, the modulus for PE was recalculated for two constrained cases: one in which the angles were held fixed so the *c*-axis strain could only come from changes in the bond length, and one in which the bond lengths were held fixed so that *c*-axis strain could only come from changes in the bond angles. The potential curves for these two cases are shown in Fig 9. The difference between these two potentials is seen to be small. The bond extension modulus obtained is 525 GPa, and the bond angle modulus is 508 GPa. The difference between these two values is within the accuracy of the calculation. This result is consistent with the previous one, that there is a small difference between bond angle deformation and bond length extension. However, both restricted deformations are stiffer than the fully free deformation, 520 GPa to 400 GPa. The substantial difference in the constrained and unconstrained moduli can be explained by the fact that bond lengths and bond angles are not independent variables in a quantum mechanics calculation, but are manifestations of the minimum energy electronic structure of a molecule.

Simulations of the X-ray diffraction patterns were also performed as a check on the strain dependent PE geometries. The crystal structure of PE is shown in Fig 10. Crystal PE is orthorhombic,  $P_{nam}$  symmetry, with unit cell dimensions of  $a=7.417 \text{ \AA}$ ,  $b=4.954 \text{ \AA}$ , and  $c=2.534 \text{ \AA}$ . Because there are two chains per unit cell, the cross sectional area is  $(a \times b) / 2$ . The location of the (006)  $2\theta$  reflection peak of the  $C_6H_{12}$  cluster describes plane spacing only along the chain axis; because an infinite number of

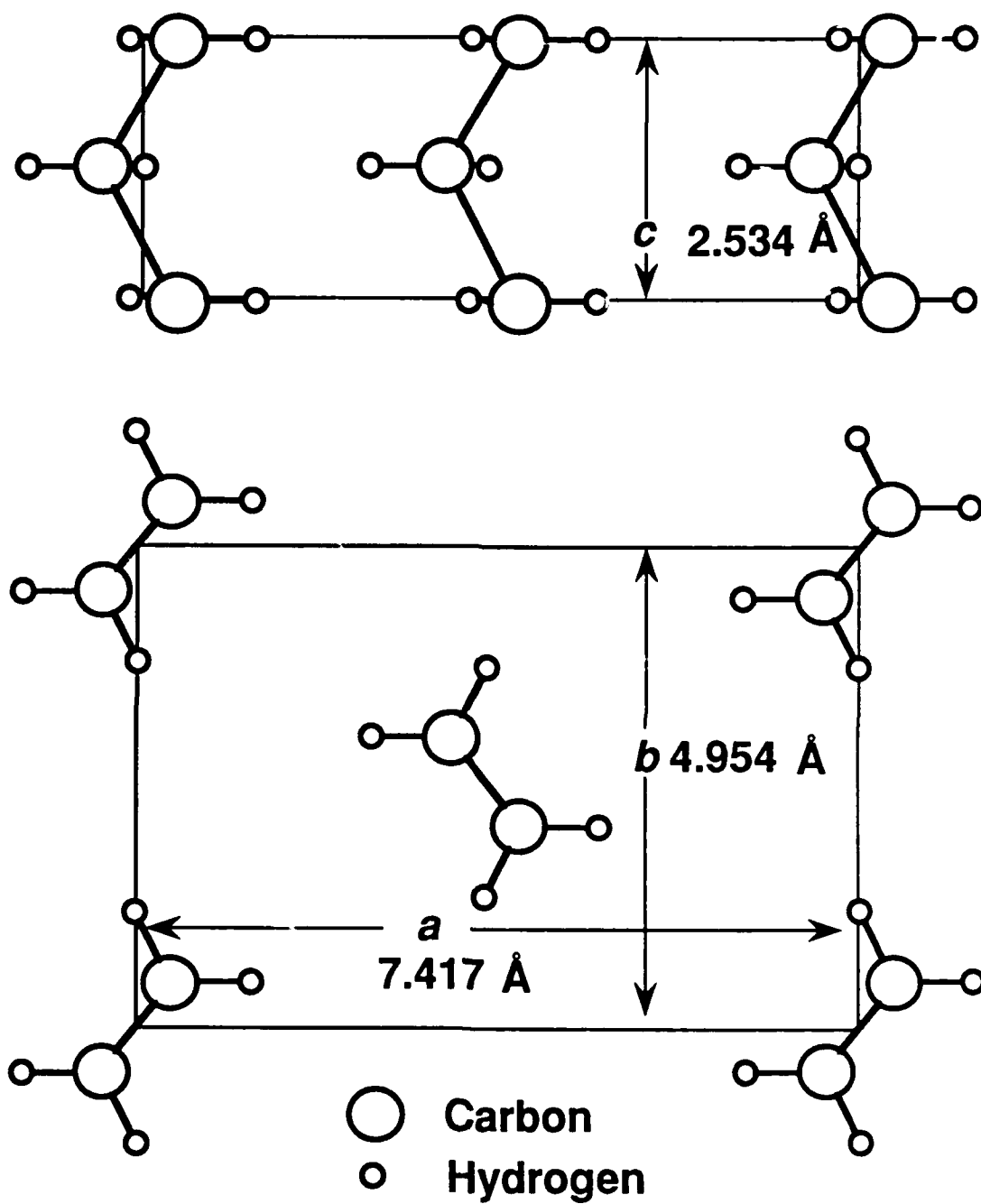
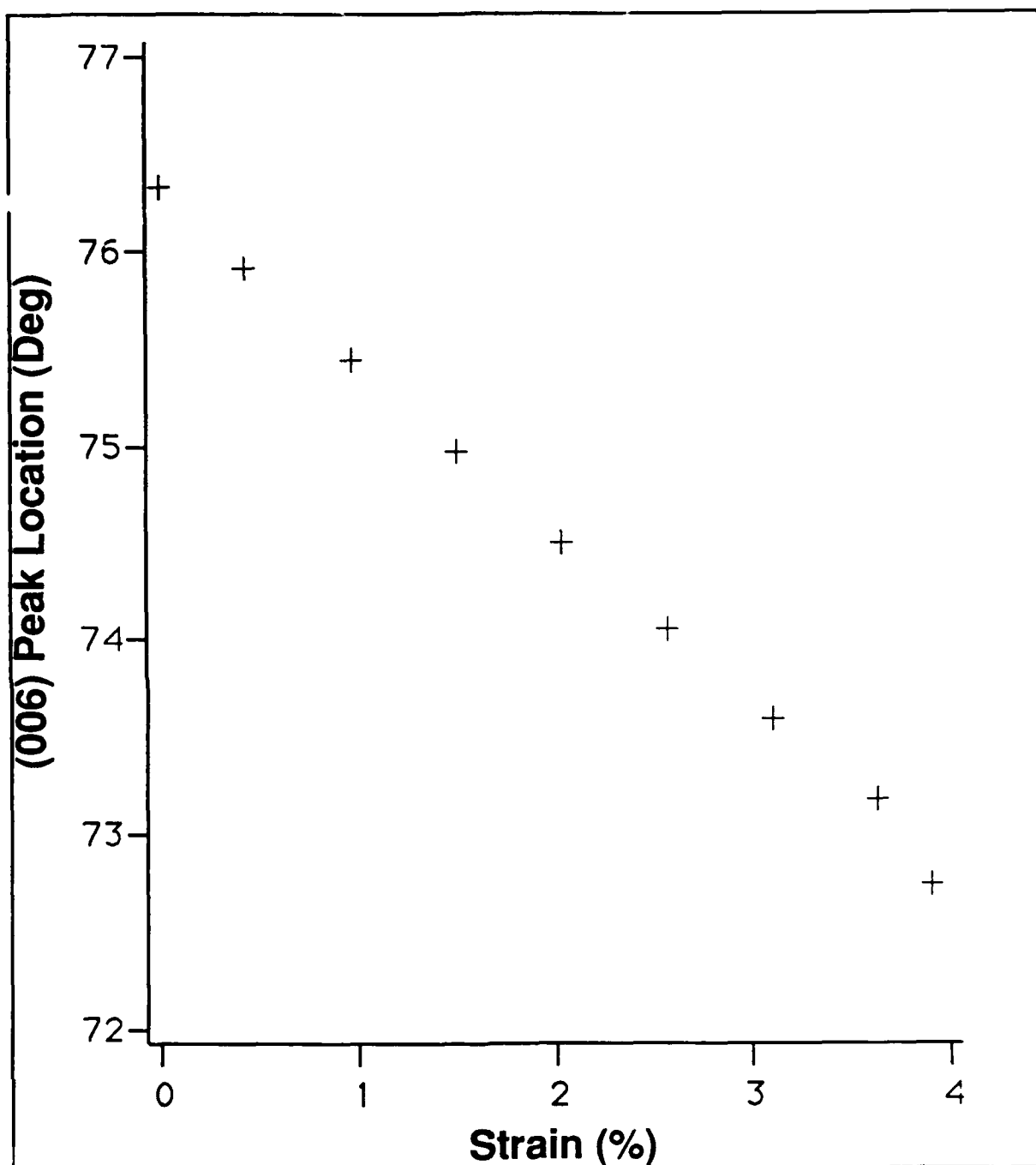


Figure 10. PE crystal structure . Here  $c$  is used as the polymer axis.



**Figure 11.** Location of 006 X-ray diffraction peak as a function of *c*-axis strain.

combinations of bond angles and bond lengths can produce the same spacing along the chain axis, the (006) peak location alone cannot be used to infer information about PE deformation. The location of the (006) reflection as a function of strain is shown in Fig 11. The modulus can be calculated from the relation

$$\epsilon = \frac{\Delta \text{stress}}{\frac{\Delta d}{d}} \quad (12)$$

where

$$d = \frac{\lambda \text{ (X-ray)}}{2 \sin(\frac{2\theta}{2})} \quad (13)$$

The X-ray modulus calculated for PE is 400 GPa, which is consistent with the modulus calculated from the second derivative of the AM1 potential. Since the first derivative of this potential is used to define the stress curve, the X-ray simulation is really just a consistency check, not an independent calculation of the modulus.

### Comparisons with Spectroscopy

The calculation of the vibrational spectra of a PE oligomer is more complicated than the spectra of a PE polymer chain because the number of degrees of freedom is much larger in an oligomer than an infinite, periodic chain. A gas phase molecule with  $n$  atoms has  $3n - 6$  vibrational modes. Thus the  $C_6H_{14}$  oligomer used for comparisons with ab-initio calculations

has 54 ( $3 \times 6$ ) vibrational modes in its spectra. The infinite PE single chain has 14 ( $3 \times 6 - 4$ ) genuine vibrations corresponding to the six atoms in the  $C_2H_4$  repeat unit, where three translations and one rotation about the chain axis do not result in vibrations.<sup>14</sup> Many of the vibrational modes in the oligomer are nearly the same, but because the oligomer is finite, the energies of these modes are not degenerate as they are in the infinite polymer. The experimental and calculated vibrational frequencies for the  $C_6H_{14}$  oligomer are listed in Table 3. Both the observed frequencies and valence force field (molecular mechanics) calculated frequencies are taken from Snyder and Schachtschneider.<sup>28, 29</sup> The behavior of the vibrational spectra of the  $n-CH_2$  series is also thoroughly discussed in these references. It is seen that the valence force field calculation agrees very well with the observed spectrum, which is not too surprising since this approach uses force constants which are obtained from spectra. The SE calculated frequencies tend to be systematically higher than observed. The ab-initio calculated frequencies agree better with the observed frequencies; however, the agreement is not as good as can be obtained using ab-initio methods because electron correlation was not included in this calculation. Even without correlation, this ab-initio calculation required in excess of 250 hours on an Elxsi mini-supercomputer, while the SE calculation only took about 16 minutes on a Silicon Graphics workstation.



**TABLE 3**  
**COMPARISON OF OBSERVED AND CALCULATED C<sub>6</sub>H<sub>14</sub>**  
**VIBRATIONAL FREQUENCIES**

OBSERVED	[cm <sup>-1</sup> ] Valence Force Field	CALCULATED [cm <sup>-1</sup> ]	
		SE AM1	Ab-Initio
---	61	55	-244
---	94	71	-243
---	125	101	81
---	139	156	107
---	208	160	135
---	216	166	170
---	303	336	312
373	370	415	374
---	474	509	495
721	723	747	746
---	740	788	786
798	798	863	895
886	887	954	922
---	894	989	977
896	896	1013	993
996	1000	1028	1027
1010	1009	1182	1062
1041	1036	1197	1070
1067	1064	1198	1103
1060	1065	1207	1137
1143	1145	1219	1190
---	1178	1225	1245
1225	1226	1226	1273
1242	1242	1237	1318
---	1277	1261	1346

TABLE 3 (continued)

OBSERVED	[cm <sup>-1</sup> ]	CALCULATED [cm <sup>-1</sup> ]	
		Valence Force Field	SE AM1 Ab-Initio
1302	1302	1264	1371
1302	1303	1312	1378
1302	1303	1369	1391
1353	1356	1394	1431
---	1368	1394	1439
1370	1372	1396	1495
---	1397	1396	1496
1450	1444	1405	1559
1452	1448	1408	1564
1462	1458	1408	1571
1463	1462	1411	1573
---	1462	1432	1574
1463	1463	1439	1577
---	1470	1444	1586
1475	1474	1458	1589
2850	2852	3002	3024
2851	2855	3012	3030
---	2858	3025	3048
2871	2862	3037	3050
2875	2882	3062	3059
2885	2882	3062	3061
---	2915	3064	3062
2907	2919	3064	3073
2920	2924	3078	3093
2934	2929	3088	3103
2965	2965	3098	3137
2965	2965	3107	3137
2965	2965	3157	3148
2965	2965	3157	3149

Using the cluster method, the spectra is calculated as though the cluster represented one repeat unit of a polymer. Thus, for PE, the cluster method assumes that the repeat unit is  $C_6H_{12}$  and not the correct  $C_2H_4$ . Thus 51,  $3n-3$ , vibrational frequencies are calculated (the mode corresponding to rotation around the chain axis is not discarded in the SE calculation). If a one repeat unit cluster were long enough to meet the criterion for noninteraction for the cluster method discussed earlier, the calculated spectra could be more readily matched with the measured chain spectra.

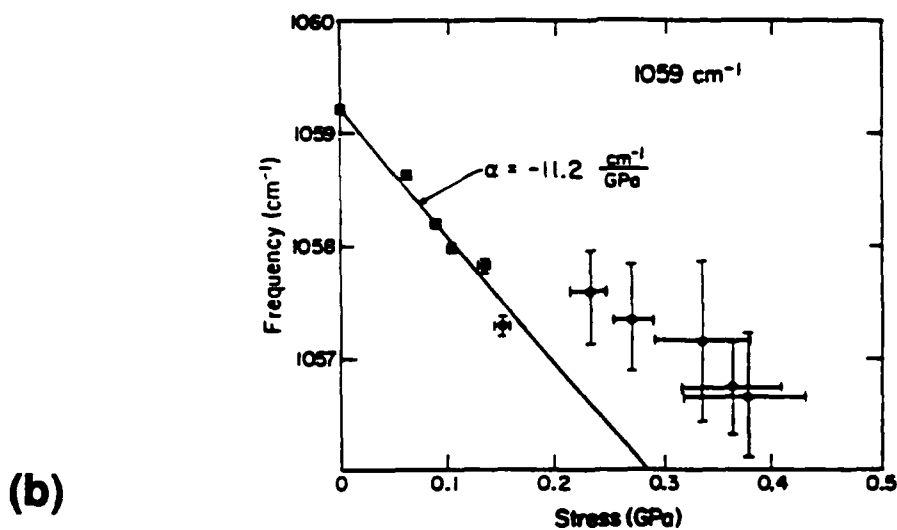
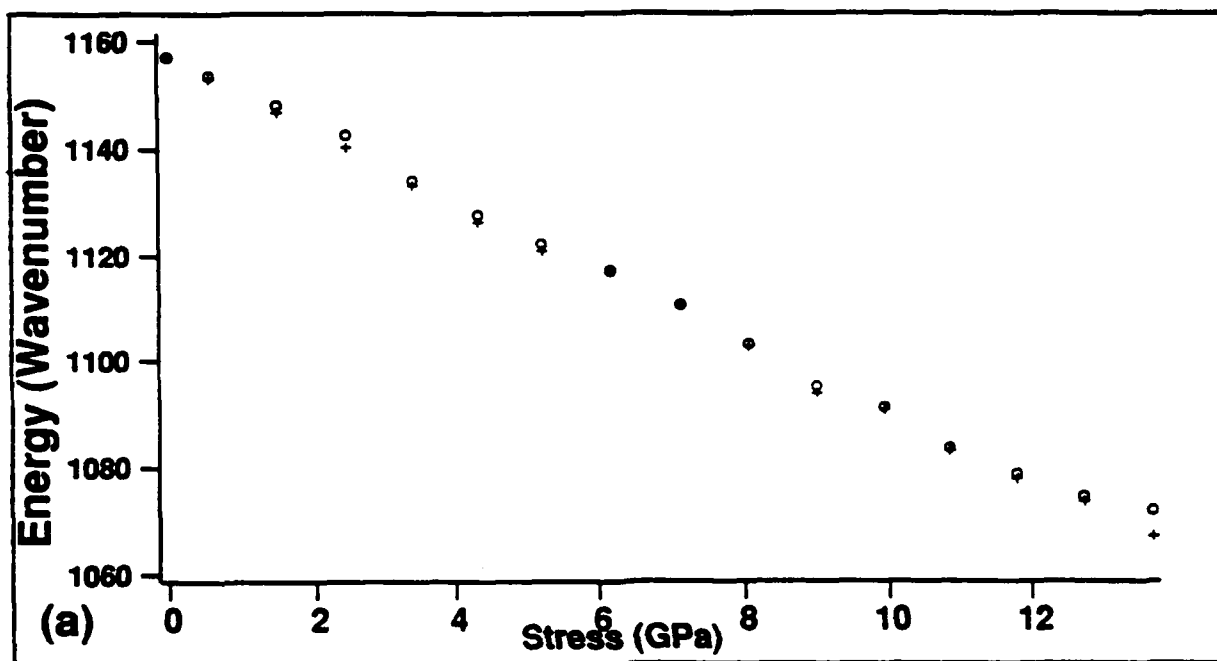
Since the periodic boundary conditions require that the PE cluster contain at least 3 repeat units, the vibrational spectrum for the cluster is much more complicated than the PE polymer spectrum. Many of the cluster vibrations involve C-H bends and stretches, which should not be very sensitive to changes in the backbone structure of PE caused by strain, and will have a minor effect on the chain modulus. In order to make the analysis tractable (for this study), the strain dependent shift of only those vibrational modes which are directly involved in backbone deformation (C-C stretch modes) and can be unambiguously matched with observed PE chain vibrational modes (by matching normal coordinates ) will be discussed in detail.

In the MOPAC calculation, one specifies the length of the (PE) cluster, thus one calculates the strain dependent properties of the cluster, here the strain dependent frequency shifts. Experimental frequency shifts are reported either as a function of strain or stress, but typically do not report stress-strain curves. The MOPAC calculated strain dependent frequency

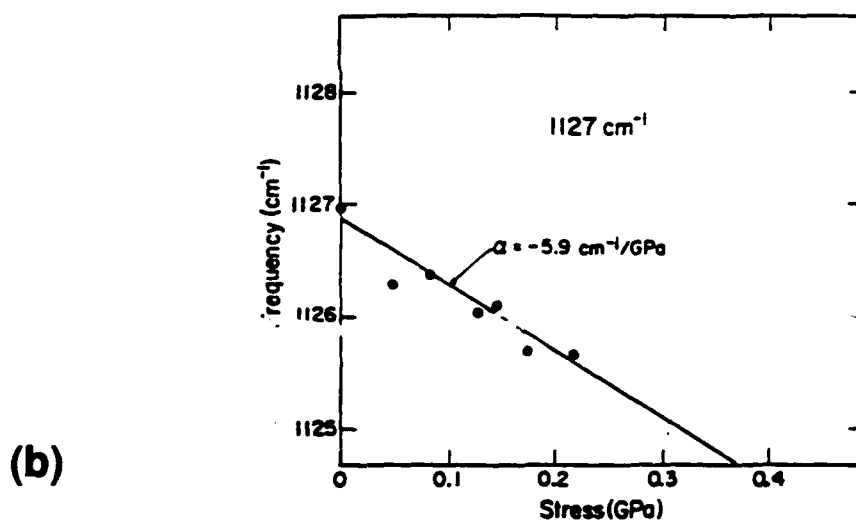
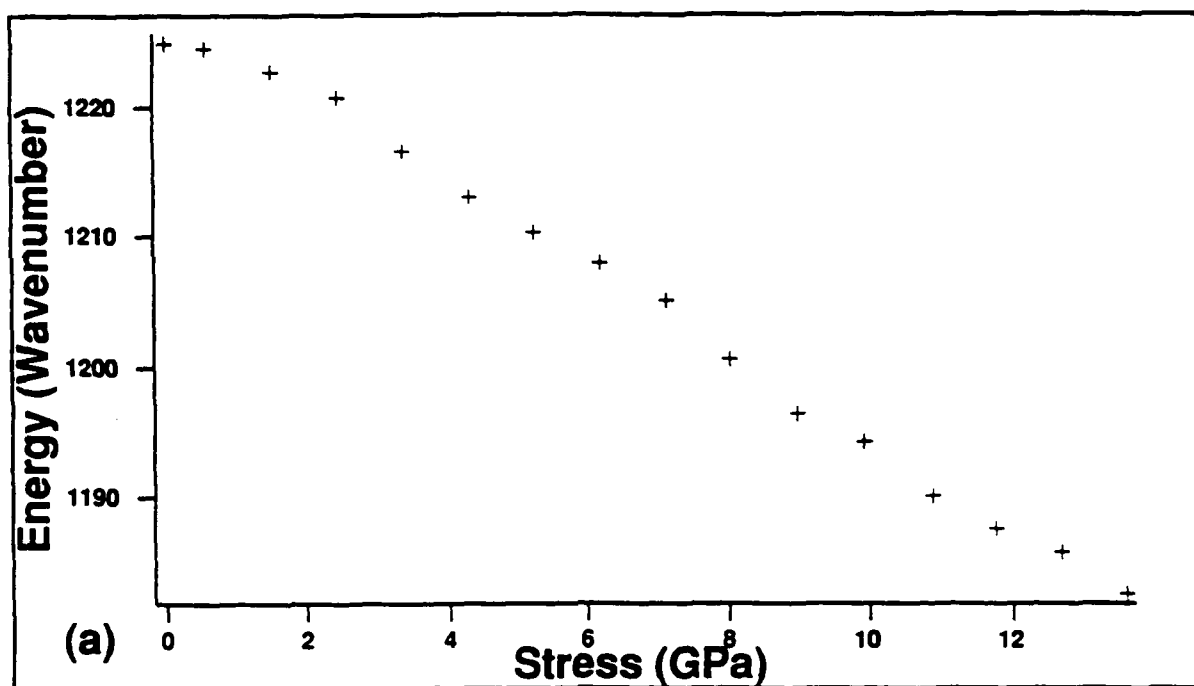
shifts can be converted to stress dependent shifts using the calculated force curve (first derivative of the heat of formation potential) to determine the proportionality between calculated strain and stress.

Figure 12a shows the stress dependent frequency shift of the two symmetric Raman active C-C stretch modes in the 3 repeat unit PE cluster. (In the infinite chain these modes are degenerate.) The observed equilibrium (zero strain / zero stress) frequency for this mode is  $1059\text{ cm}^{-1}$ , while the SE calculated frequency is  $1157\text{ cm}^{-1}$ . The calculated shift of these lines is linear out to a stress of 14 GPa (4% strain) with a slope of  $-5.86\text{ cm}^{-1} / \text{GPa}$  ( $-23.3\text{ cm}^{-1} / \% \text{ strain}$ ). Fig 12b, reproduced from reference 15, shows the measured stress dependent shift of this C-C stretch mode in ultra-oriented PE film. Wool<sup>19</sup> states that measured shift in the low stress region is considered more representative of the value obtained under the assumption of uniform stress on the chains. Deviation from linearity in the calculated stress dependent shift is not observed because stress is (inherently) uniformly applied in the calculation independent of the amount of stress applied. Because strain is proportional to stress, the fact that the calculated stress dependent frequency shift is 0.52 times the measured shift means that the calculated strain dependent frequency shift is 1.92 ( $1 / 0.52$ ) larger than the strain dependence of the measured frequency shift.

Figure 13a shows the calculated stress dependent frequency shift of the asymmetric C-C stretch modes in PE. Because this is an asymmetric stretch, only one frequency is present with the correct normal coordinates.



**Figure 12.** PE asymmetric C-C stretch mode stress dependent shift (a) AM1 calculated (b) experimental. The calculated stress dependent shift is roughly one-half the experimental shift, which means the calculated strain dependent shift is roughly twice the experimental



**Figure 13.** PE symmetric C-C stretch mode stress dependent shift (a) AM1 calculated (b) experimental. The calculated stress dependent shift is roughly one-half the experimental shift, which means the calculated strain dependent shift is roughly twice the experimental

The experimental zero strain frequency for this mode is  $1127\text{ cm}^{-1}$ , while the SE calculated frequency is  $1224\text{ cm}^{-1}$ . The calculated shift of this mode is  $-3.3\text{ cm}^{-1}/\%$  strain,  $-2.88\text{ cm}^{-1}/\text{GPa}$ . Figure 13b, reproduced from reference 14 shows a measured shift of  $-5.9\text{ cm}^{-1}/\text{GPa}$ . The calculated strain dependent shift rate is 2.04 times the observed strain dependent shift rate.

A possible explanation for the difference in the calculated and observed strain dependent frequency shifts might be that the measured bulk strain is not be completely taken up in *c*-axis chain strain. If the stress applied to PE were roughly equally partitioned between chain slippage and chain extension, only one-half of the bulk strain would be *c*-axis strain, and the calculated frequency shifts would agree with the measured shifts. This hypothesis was investigated by calculating the interaction energy of two PE chains (inter-chain friction) packed in the crystal structure. The program Cerius<sup>30</sup> for Silicon Graphics workstations was used for this crystal simulation. A standard Lennard-Jones potential with an interaction radius of  $5\text{ \AA}$  was used to describe the non-bonded interactions between two PE chains. The equilibrium geometry obtained from the AM1 calculations was used for the PE chains. One PE chain was moved along the *c*-axis of the crystal with respect to the other, and the change in energy monitored. As expected, the interaction energy increased as the chains were slipped against each other; the energy was periodic with a period equal to the repeat unit length. The energy barrier to chain slippage was found to be approximately 2% of the chain axis barrier. This means that under strain

amorphous PE will initially deform by chain slippage rather than by extension of the chains themselves . ( This behavior has been observed in unoriented PE. <sup>31</sup>) Because the resistance to chain slippage is so much smaller than the chain resistance, equipartition between inter and intra molecular potentials cannot be invoked to explain the discrepancy between the measured and calculated frequency shifts.

Since the discrepancy in frequency shifts cannot be explained by inter-molecular interactions, the next logical step is to investigate the validity of the intra-molecular interactions, i.e., the bonding potentials. Wool <sup>17</sup> performed a analysis of the strain dependent frequency shifts of PE. In addition to very thorough measurements, he also calculated PE deformation using a molecular dynamics model. The Morse potential shown in Figure 14 was used to describe the C-C bonds in PE. In this reference, the source for the parameters in the C-C Morse potential is not listed, however, these parameters are essentially identical to those used in similar models found in other references<sup>24</sup>. Because Wool's model matches both the equilibrium frequencies and the strain dependent frequency shifts for all the PE chain vibrations which were intense enough to be reliably measured, this description of the C-C bond in PE is judged to be accurate.

The C-C bond strain potential which arises from the AM1 parameters was obtained by varying the C1-C2 bond distance in the PE cluster shown in Fig 5 and allowing all the other variables to optimize. This potential is also shown in Fig 14 from -25 % to 50% strain. In this figure it is seen that the



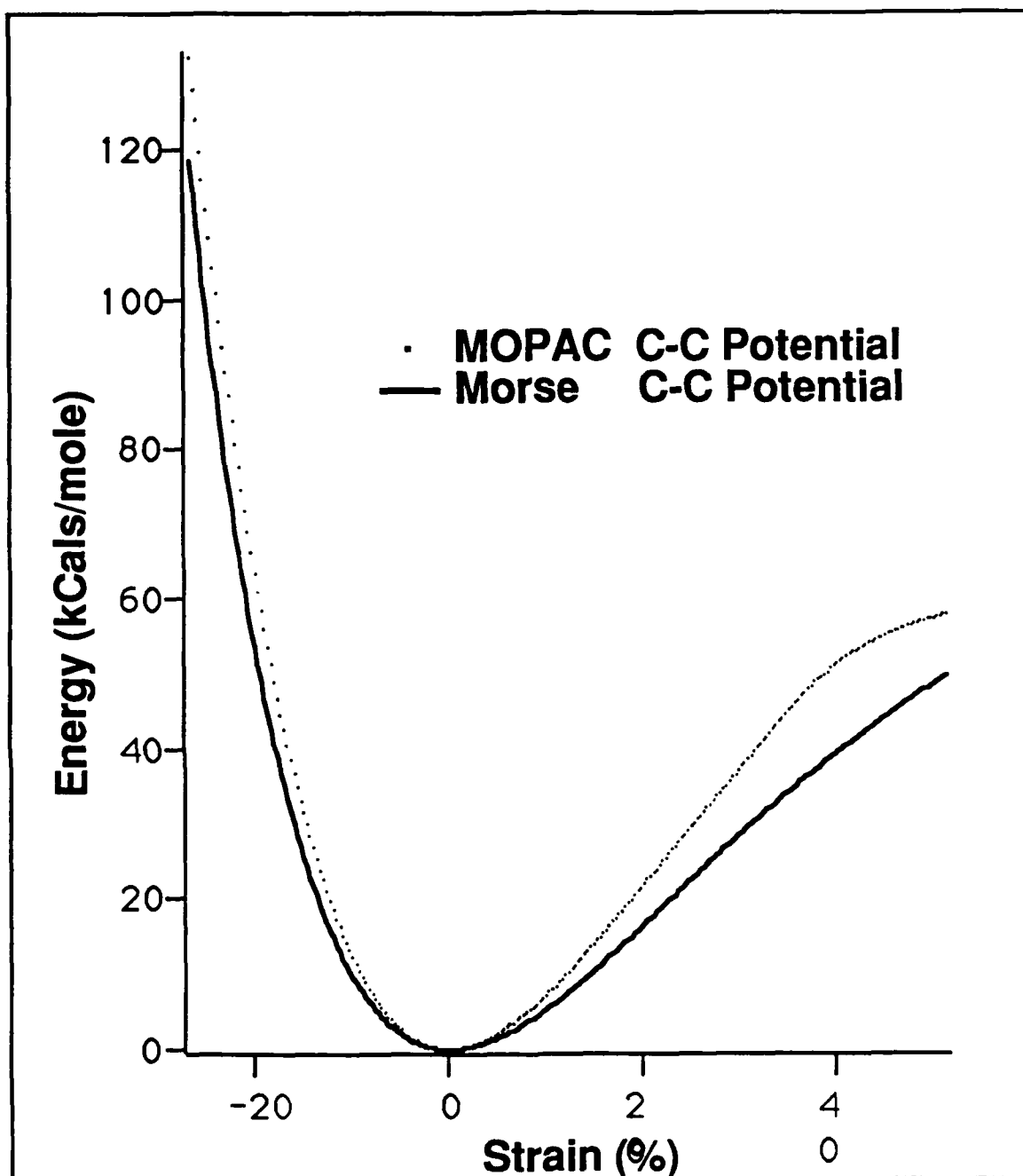
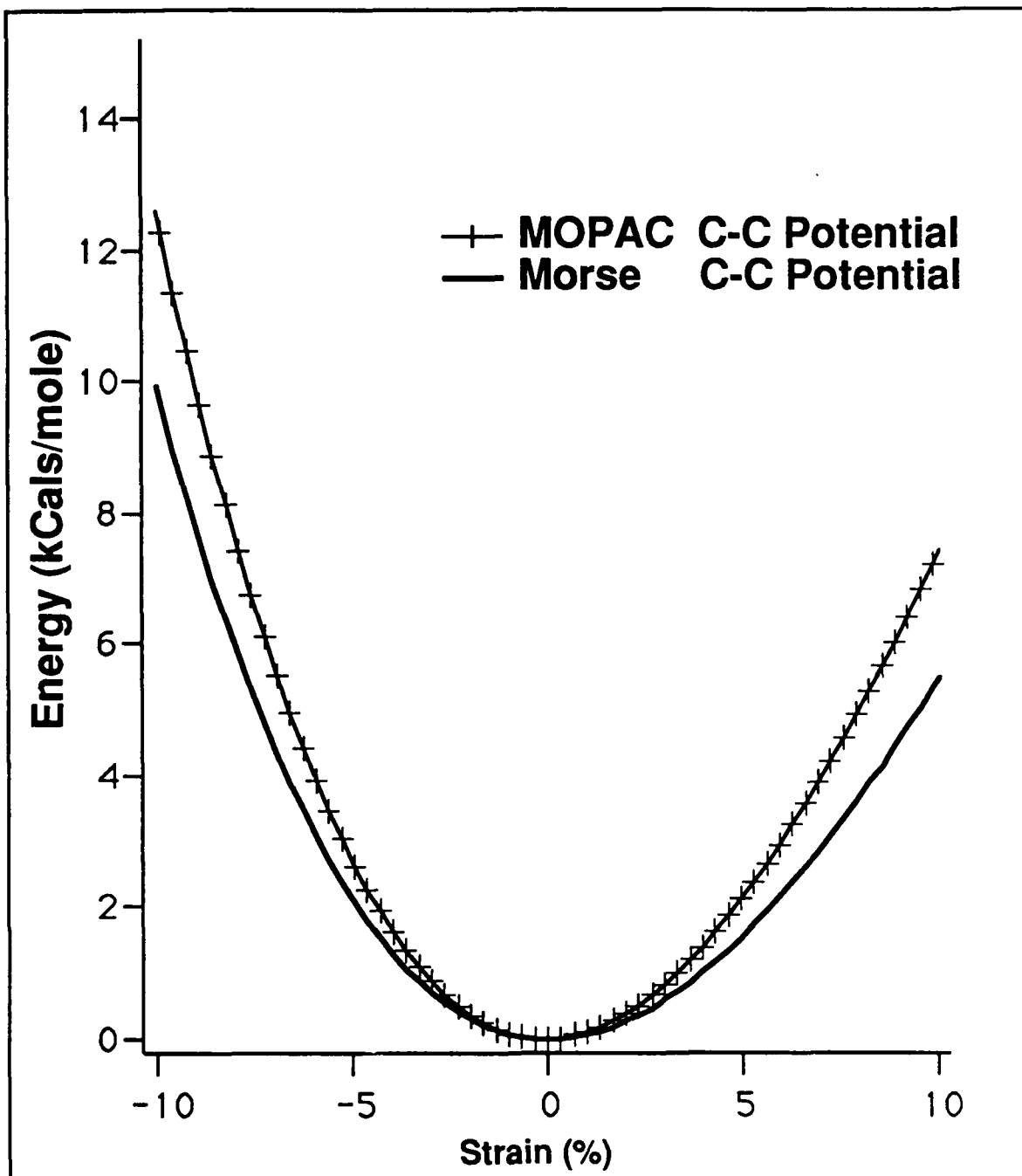


Figure 14. Comparison of Morse and AM1 C-C strain potentials.



**Figure 15.** Comparison of Morse and AM1 C-C strain potentials: expanded view about equilibrium.

AM1 C-C potential is systematically higher in energy than the Morse potential. An expanded view around equilibrium is shown in Fig 15, which shows that there is a significant difference in the two potentials even for small variations about equilibrium. The second derivative of the AM1 C-C potential at equilibrium is  $580 \pm 20 \text{ Nt / m}$ , which is 31% stiffer than the second derivative of the Morse C-C potential at equilibrium,  $440 \text{ Nt / m}$ .

The effective CCC bond angle potential can be obtained by varying angle C1-C2-C3 (Fig 5) and allowing the rest of the cluster to optimize. A value of  $1.566\text{e-}18 \text{ Nt m / rad}^2$  was obtained for the angle bending force constant calculated by the AM1 Hamiltonian. A force constant for a CCC angle bend of  $1.084\text{e-}18 \text{ Nt m/rad}^2$  was used in reference 27. Again, the value from AM1 is approximately 30% higher than has been empirically found to predict the correct frequencies and frequency shifts.

Wool reports a value of 267 GPa for the chain modulus of PE based on his measurements and modelling, which differs by -10% from the "accepted" value of 300 GPa for PE. The AM1 result was 400 GPa, which differs from the "accepted" value by +33%. The frequency shifts predicted by AM1 are roughly a factor of two larger than experimentally observed. The Morse potential used by Wool has second and third derivatives that agree with experiment. The C-C bond potential generated by the AM1 parameterization is judged to be inaccurate because its derivatives are larger than experimentally observed, hence the modulus, which depends directly in the second derivatives of the potentials, is judged to be inaccurate; however it is premature to assign a quantitative error in the

AM1 calculation of polymer modulus based only on these results.

## V POLYDIACETYLENE RESULTS AND DISCUSSION

### Substituent Effects

Polydiacetylene (PDA) is one of a few polymers which can be polymerized as a single crystal. The backbone chain structure, shown in figure 16, is simple; however, the substituents (indicated by R in figure 16), are typically large structures containing up to 30 atoms (including hydrogens). If one considers a "ball and spring" mechanical model of PDA, it seems reasonable to assert that the stiffness of the polymer along its *c*-axis should be independent of substituent because the substituent spring (bond strength) is orthogonal to the chain axis. In reality, the bond between the backbone and the substituent will affect the bonding on the backbone, but unless the backbone is bonded to a halogen atom, the influence on backbone bonding should be small. One could argue that the conjugated PDA backbone determines the chain stiffness; however, because the substituent's size determines the crystal packing density hence the unit cell cross sectional area, substituent geometry ultimately determines the modulus.

If this argument were valid, the PDA derivative which has the substituents which give the best crystal packing (highest density) would have the largest modulus. Table 4 shows a comparison of 4 PDA variants whose chemical formulae are listed in figure 16. (PDA derivatives are commonly referred to by only the substituent type; for clarity in this thesis I will add the abbreviation PDA. For example, PDA-EUHD referred to herein is referred to simply as EUHD in the literature). PDA-EUHD,



which has the smallest unit cell area also has the largest mechanical modulus. Because all the substituents listed have a carbon atom bonded to the backbone their effect on the backbone bonding should be the same. The last column in Table 4 lists the product of the modulus and the derivative's cross sectional area, the chain restoring force which is the chain stiffness times the repeat unit length. The restoring force is seen to be independent of substituent to within experimental accuracy.

TABLE 4  
COMPARISON OF PDA DERIVATIVE PROPERTIES<sup>32</sup>

<u>Derivative</u>	<u>Area [<math>\text{\AA}^2</math>]</u>	<u>Modulus [GPa]</u>	<u>Restoring Force [<math>10^{-8}</math> Nt]</u>
PUHD	97.4	45 M	4.38
TSHD	95.5	43 M 50 R	4.11 4.75
DCHD	106.3	45 M 47 B	4.78 4.95
EUHD	65.1	61 M 74 R	3.97 4.79

M: Mechanical measurement of modulus  
R: Raman measurement of modulus from acoustic velocity in polymer  
B: Brillouin measurement of modulus

Ref 32 does not give the uncertainties in the modulus measurements which are taken from a number of experiments (which are referenced in this paper), but an uncertainty of  $\pm 5$  GPa is typically quoted in similar

experiments.

The weak dependence of PDA modulus on substituent is very important for this study because for every 4 carbon atoms in the backbone repeat unit, there are as many as 50 substituent atoms. The vast majority of the computation time would be spent optimizing the geometry of the substituents, and the number of calculated vibrational frequencies would grow very large and needlessly complicate the analysis of the spectrum since the substituent frequencies would be interspersed with the strain dependent backbone frequencies. More importantly, since the computational cost scales as  $n^2$  (number of electrons), the MOPAC calculations would have been too slow to be useful. Instead of calculating the real polymers, PDA with hydrogens as substituents was considered in the majority of the work performed in this study. This is a good model for comparison because molecular mechanics models of PDA derivatives often treat the substituents as a single atom with a mass equal to the mass of the entire substituent in order to obtain a good match of the vibrational coupling to the backbone.<sup>33,34,35,36</sup> In order to investigate isotope effects, MOPAC 5.0 allows the user to specify the masses of the atoms, e.g., specifying a hydrogen atom with mass 2.0 changes the hydrogen to deuterium. MOPAC 5.0 does not restrict the user to naturally occurring isotopes; an arbitrary mass can be assigned to any atom. This flexibility was exploited to match the empirical models by attaching very heavy hydrogen atoms to PDA. For example, to match the model of PDA-HHD used in reference 33, mass 31.26 atomic mass units (amu) and 15.12 hydrogen atoms were used as



substituents. The mass of the atoms does not affect the calculated minimum energy geometries because in the Hartree-Fock method the solution of the electronic wavefunctions is independent of the nuclear wavefunctions. This was verified for MOPAC 5.0 by calculating the optimum geometry of a simple molecule while varying the masses of the hydrogen atoms in the molecule. Even with mass  $10^6$  amu hydrogen, all of the variables, bond lengths, angles, etc, were exactly the same (to machine precision).

### Molecular Structure

An SE polymer molecular structure calculation on PDA has not been previously performed, so the first step in this study was to determine the minimum cluster length. The minimum cluster length was determined by examining the heat of formation per repeat unit and *c*-axis length as a function of the number of repeat units in the cluster. The results are summarized in Table 5. These results indicate that the normalized heat of formation and *c*-axis length reach their asymptotic values with a 4 repeat unit cluster, which is used for all polymer calculations. For comparison, Table 6 lists similar results for the PDA oligomer sequence. The oligomers demonstrate behavior similar to the cluster sequence. The decrease in heat of formation per repeat unit from 1 to 2 occurs because an extra carbon is included in the one repeat unit case to match the polymer *c*-axis.

TABLE 5

## PDA CLUSTER SERIES

n: C <sub>4</sub> H <sub>2</sub>	Heat of Formation ( $\Delta H_f$ ) [kCals/mole]	$\Delta H_f / n$ [kCals/mole]	Cluster Length [Å]	Repeat Unit Length [Å]
1	77.68	77.68	4.708	4.708
2	127.21	63.60	9.753	4.876
3	186.51	62.17	14.634	4.878
4	247.94	61.98	19.505	4.876
5	309.83	61.96	24.382	4.876
6	371.76	61.96	29.282	4.880
7	433.66	61.95	34.122	4.874

TABLE 6

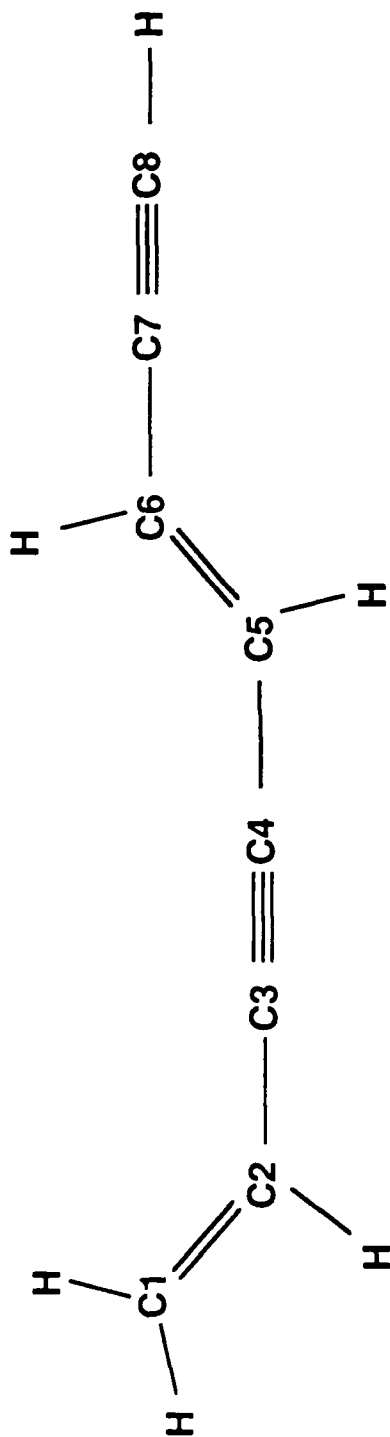
## PDA OLIGOMER SERIES

Formula [kCals/mole]	n Repeat Units	$\Delta H_f$ [kCals/mole]	$\Delta H_f (n) - \Delta H_f (n-1)$
C <sub>5</sub> H <sub>6</sub>	1	56.30	----
C <sub>8</sub> H <sub>8</sub>	2	95.92	39.62
C <sub>12</sub> H <sub>10</sub>	3	158.55	62.63
C <sub>16</sub> H <sub>12</sub>	4	220.59	62.04
C <sub>20</sub> H <sub>14</sub>	5	282.53	61.94
C <sub>24</sub> H <sub>16</sub>	6	344.46	61.93
C <sub>28</sub> H <sub>18</sub>	7	406.40	61.94

A 4 repeat unit oligomer of PDA with hydrogen substituents is too large even for a low level ab-initio calculation. A smaller PDA oligomer shown in figure 17 was used for comparisons between ab-initio and SE calculations. Also listed are geometric values from a 4 repeat unit cluster with methyl ( $\text{CH}_3$ ) substituents and an experimental X-ray diffraction determination of PDA-THD<sup>37</sup>.

There are several notable features in the geometry of this PDA oligomer. First, the minimum energy geometry occurs with the end carbons both above (cis) the plane of the central acetylene group, while in the polymer successive repeat units are always on opposite sides of this plane (trans). In the oligomer with hydrogen substituents, the barrier to rotation was calculated and found to be very low (thermal), which means that the ends of this oligomer would freely rotate at room temperature. Steric interactions with larger substituents would restrict the rotation of the oligomer; however, in the AM1 cluster calculations with hydrogen substituents, the PDA cluster geometry always optimized in the trans configuration, which is observed experimentally for the PDA polymer. This free rotation is a significant end effect in the oligomer, and complicated attempts to calculate the modulus on a two repeat unit oligomer. (The rationale for these attempts is discussed later in this chapter.)

There are significant differences in the backbone C-C bond lengths between PDA and PE. The PDA C-C single bond is considerably shorter than both the C-C single bond in PDA, and the C-C single bond to the carbon atom in the substituent. This occurs because the backbone "single" C-C



Bond Distance [Å]	Oligomer		AM1 Cluster		PDA-THD Ref 37
	Ab-Initio	AM1	H sub.	CH <sub>3</sub> sub.	
C1-C2	1.322	1.345	1.386	1.405	1.36
C2-C3	1.428	1.396	1.379	1.407	1.43
C3-C4	1.193	1.207	1.220	1.223	1.21
C4-C5	1.424	1.392			
C5-C6	1.328	1.362			
C6-C7	1.423	1.398			
C7-C8	1.190	1.200			

Bond Angle [Deg]	Oligomer		AM1 Cluster		PDA-THD Ref 37
	Ab-Initio	AM1	H sub.	CH <sub>3</sub> sub.	
C1-C2-C3	123.57	124.07	122.80	125.20	119.1
C4-C5-C6	123.32	123.10			
C5-C6-C7	123.01	123.54			

**Figure 17.** PDA geometry, calculated for the oligomer shown, for a 4 repeat unit cluster with hydrogen and methyl substituents, and values obtained from X-ray diffraction measurements.

bond is really a mixture of a single C-C bond and a triple C-C bond. This bond is somewhere between a pure C-C single bond with a length of 1.53 Å and a pure C-C double bond with a length of 1.326 Å. The AM1 calculation predicts that the C-C double bond (C1-C2) and C-C single bond (C2-C3) in PDA have nearly equal lengths; the ab-initio calculation shows these bond lengths to differ measurably, which agrees much better with experiment than the SE results. The error in these AM1 bond lengths is larger than the average error in bond lengths as listed in Table 2, which may show a limitation in the AM1 parameterization for conjugated carbon bonds. The C-C triple bond lengths calculated by AM1 and ab-initio both agree very closely with experiment. The bond angles calculated by AM1 are within the published accuracy of this method. An earlier MNDO calculation on a one repeat unit PDA oligomer with methyl substituents showed results which were more consistent with the experimentally observed geometry.<sup>38</sup> A MNDO calculation on the oligomer shown in Fig 17 was performed in this study and found to produce approximately the same results as the AM1 calculation.

Figure 18 shows a comparison of the distribution of strain within the PDA repeat unit as a function of *c*-axis strain. The bond angle is seen to show the largest relative change with strain. Initially the single and double C-C bonds deform at the same relative rate, but at strains greater than 4% the single C-C bond begins to change more rapidly. The triple C-C deforms very little at low strains and begins to deform linearly for strains above 2%. Overall, this behavior is consistent with what one would expect

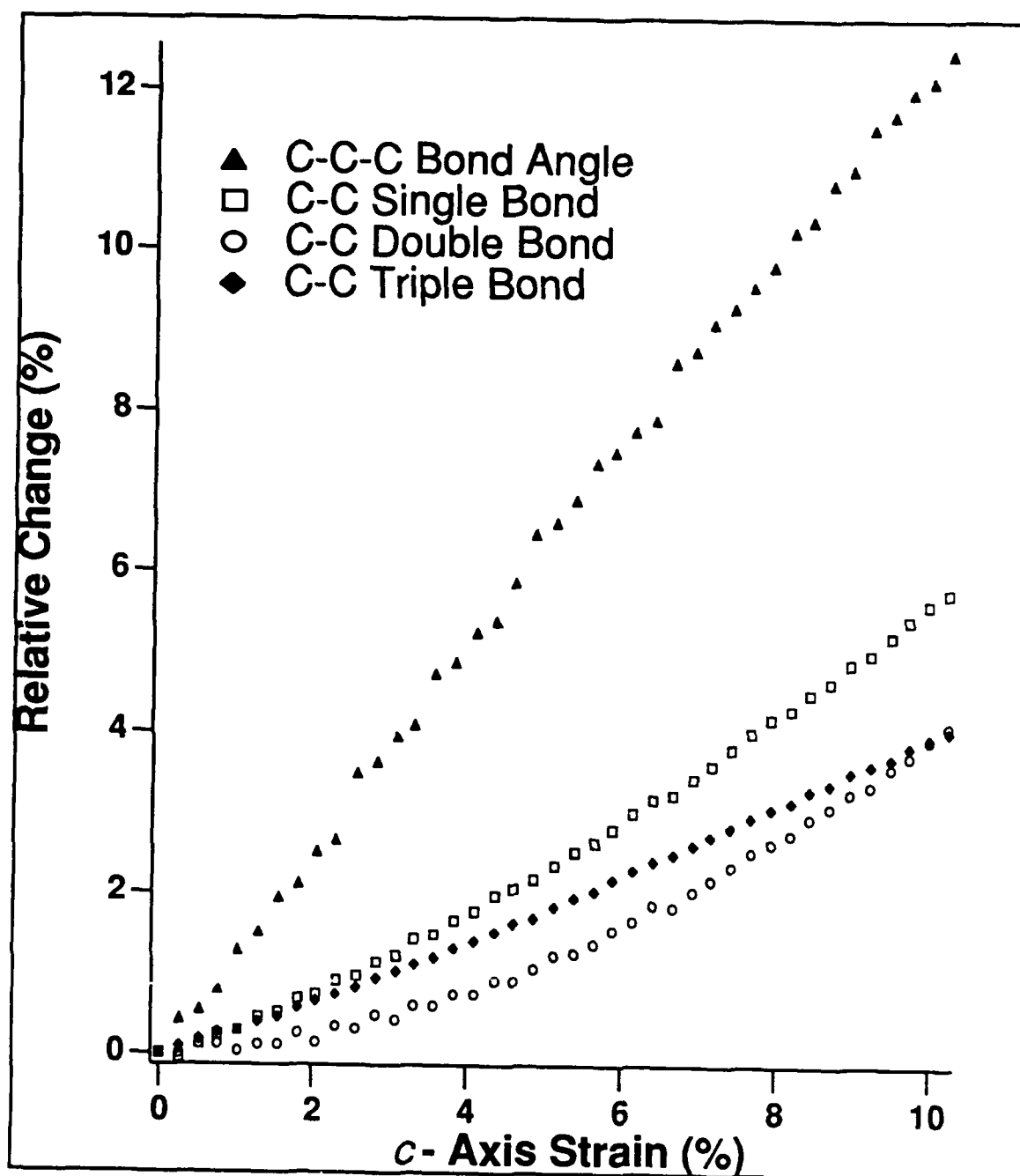


**Figure 18.** PDA distribution of chain strain among bond angle and bond lengths.

based on the anticipated stiffness of each mode, the triple bond being the strongest, the angular resistance being the weakest; however, it is interesting that the relative deformation of the PDA single and double C-C bonds is roughly equal. This result may be explained by the fact that these are not pure double and single bonds. The AM1 calculated deformation is consistent with the experimentally reported deformation of PDA-HDU, ( $R=CH_2OCONHC_6H_5$ ).<sup>39</sup>

### Modulus Calculations

The strain dependent heat of formation curves for a 4 repeat unit PDA cluster is shown in figure 19 from -5% to 10 % strain. Two cases are shown in this figure, one with hydrogen substituents and one with methyl substituents. As is seen, these potentials are essentially identical, which reinforces the argument that PDA chain stiffness is largely independent of substituent. Results below -5% were not obtained because the specification of the PDA geometry caused the optimization to fail if a bond torsion angle rotation occurred. Numerous alternate geometry specifications were attempted to work around this problem, but none were successful. Since experimental data below -4% have not been reported, this issue was not pursued. The chain stiffness obtained by the same procedure used for PE is 42 Nt/m. The AM1 calculated modulus for the PDA variants described before are listed in Table 7 along with the measured bulk values (cross sectional area are taken from Table 4). As was seen in PE, the AM1 calculated modulus is substantially higher than the measured values. Better agreement was anticipated because PDA's structure is much closer

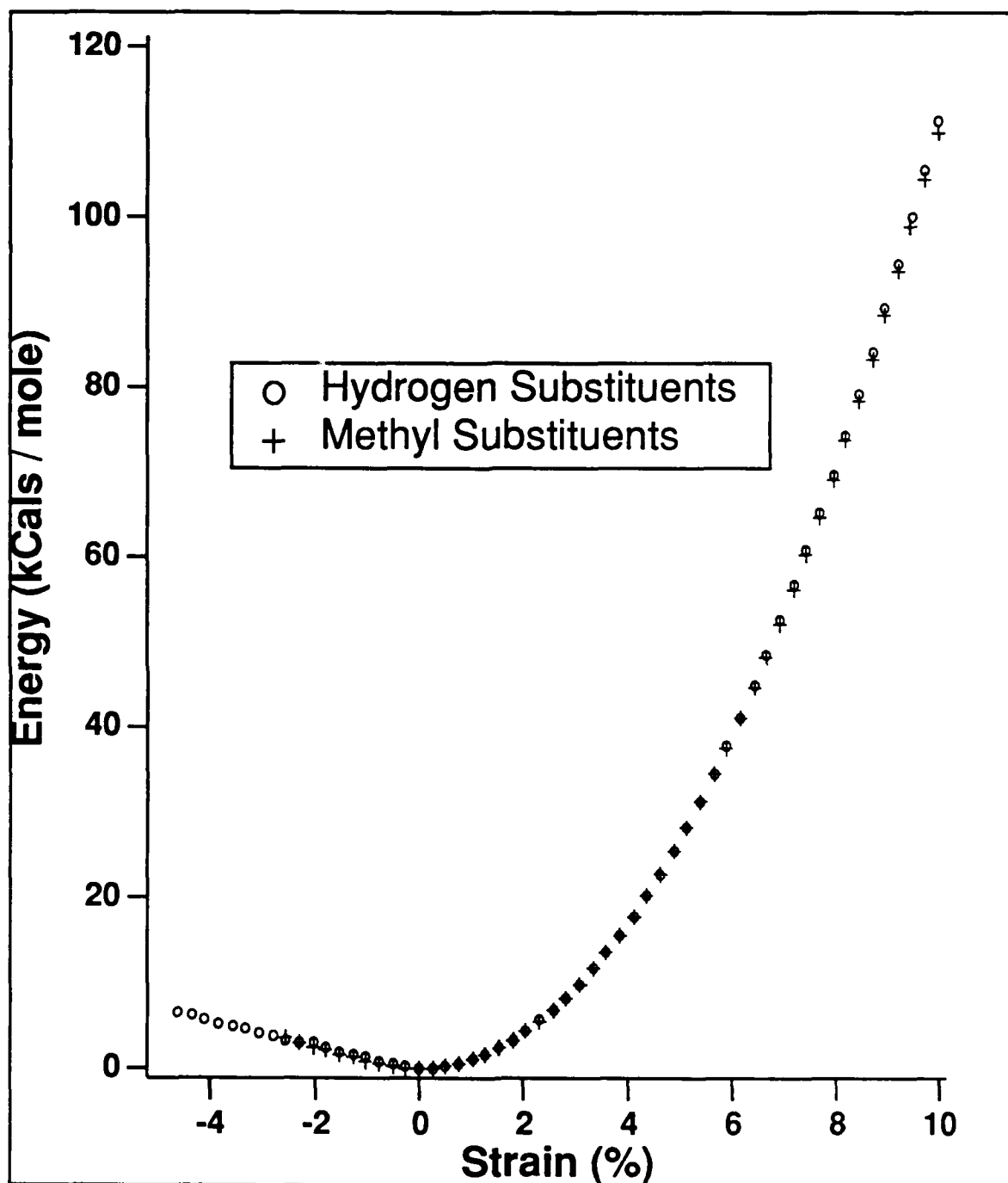


**Figure 19.** Comparison of Mopac heat of formation curve for a 4 repeat unit PDA cluster with hydrogen and methyl substituents



to the ideal chain simulated in these calculations. As was required for PE, other predictions of the AM1 calculation need to be compared with experiment to assess the accuracy of this method.

TABLE 7  
COMPARISON OF EXPERIMENTAL AND CALCULATED PDA CHAIN  
MODULUS

PDA Derivative	Experimental Modulus [Gpa] <sup>32</sup>		AM1 Modulus [GPa]
PUHD	45 M		86
TSHD	43 M	50 R	88
DCHD	45 M	47 B	79
EUHD	61 M	74 R	129

In order to discover how much of the modulus error comes from the approximations made in the AM1 method, a direct comparison of the strained geometry heat of formation calculations between the SE and ab-initio methods was planned. The ab-initio codes which was available for this study, Gaussian88 and Gaussian90, do not have provision for the use of periodic boundary conditions to simulate an infinite chain, so this comparison had to be limited to an oligomer. Because of the memory constraints, the maximum practical oligomer which could be used in the ab-initio calculation was only two repeat unit long. This oligomer is shown in figure 20. Calculations were first performed using the SE method to see

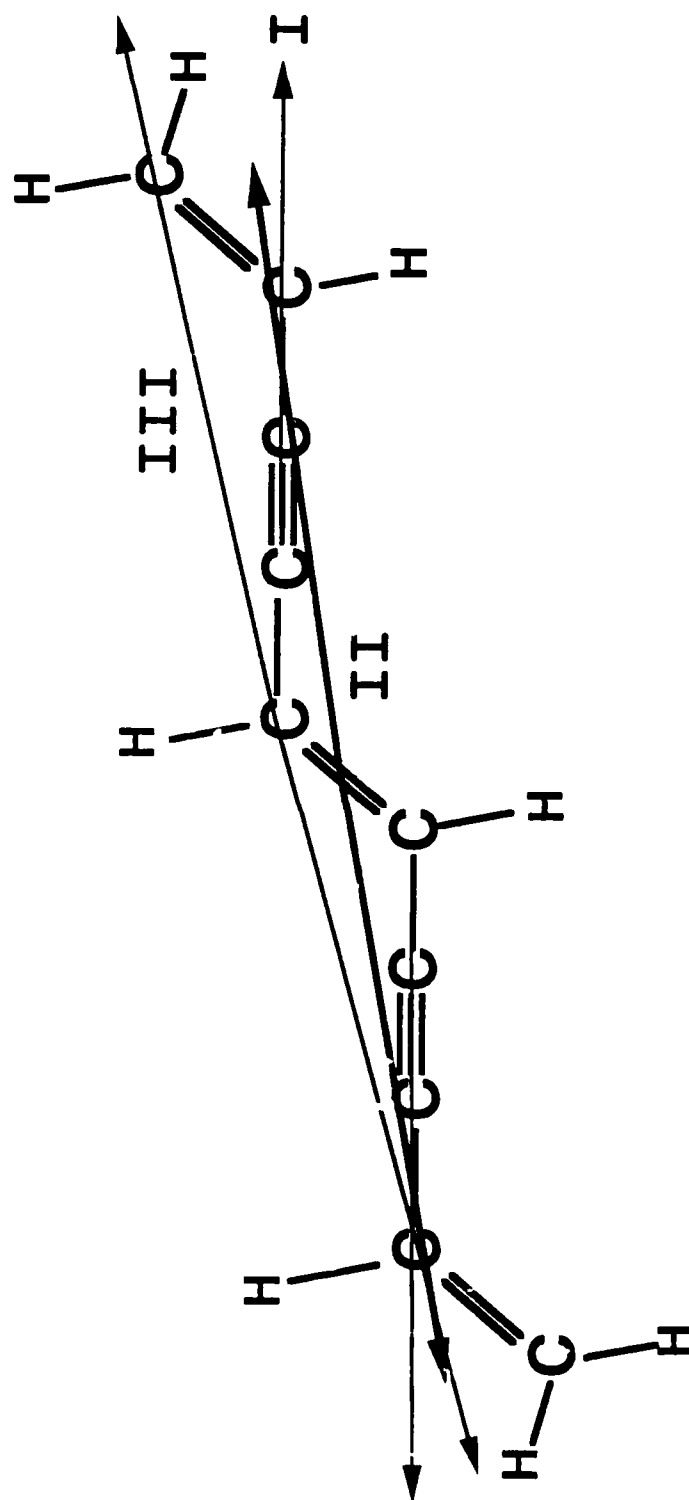


Figure 20. PDA 2 repeat unit oligomer used in strain calculations. Arrows represent vectors used in the applied strain. III corresponds to strain along the c axis.

if the effect of strain on a two repeat unit oligomer was representative of the infinite chain. Two interesting results were obtained from the SE calculations. First, the vector direction in which strain is applied affects the optimized geometry. Strain is applied in an oligomer by displacing the "end" atoms (symmetrically) a small distance away from their equilibrium location and holding them fixed. The rest of the oligomer geometry is allowed to optimize under this constraint. Because the atom locations are specified by a bond distance and angle, successive displacements take place along an effective strain vector. Several vector directions which were used are shown in figure 20. Because each successive atom displacement is very small, the actual position where the atom is placed differs minutely depending on the strain vector. Surprisingly (at least to the author), the heat of formation and optimized geometry was found to be very sensitive to the strain vector. In order to match the strain direction in the cluster method, atom displacement was specified along vector III, which is along the polymer *c*-axis. Unfortunately, the results of this calculation showed that a two repeat unit oligomer was dominated by end effects, and the comparison to the infinite chain was invalid. Therefore, the ab-initio comparison was not performed.

#### Comparisons With Spectroscopy

The accuracy of the modulus calculation of PDA, as for PE, can be investigated by comparing the measured and AM1 calculated strain dependent vibrational frequency shifts. The large, 4 repeat unit cluster required for PDA made this analysis more difficult because the normal

vibrational modes for a 4 repeat unit cluster are very different than the vibrational modes for the infinite chain. Because the substituents couple into some of the backbone chain Raman active modes, it is difficult to accurately match these modes with the hydrogen substituents. The experimental spectrum is complicated because some frequencies that arise solely from the substituents are interspersed with the chain modes. The substituent frequencies do not shift with strain, so they don't provide any information on the accuracy of the strain dependence of the AM1 calculation. After a thorough analysis, only two calculated vibrational frequencies could be unambiguously, reliably matched with the reported spectra. The normal coordinates of these modes are shown in figure 21.<sup>34,36</sup> These measurements have been performed on a variety of PDA substituents of varying degrees of polymerization, so there is considerable spread in the reported frequency shifts.<sup>40</sup>

The strain dependent frequency calculations were first performed using mass 1 amu hydrogen substituents, which produced an unrealistic spectrum because the coupling of the light mass hydrogens to the backbone vibrations was too strong. When the calculation was performed with mass 32 hydrogens, the backbone coupling better matched the experiment and the spectrum was easier to interpret. Interestingly, the frequencies of the two strongly strain dependent Raman modes were found to be independent of the hydrogen mass. A possible problem with approximating the substituents with heavy hydrogen atoms is that the bond length and the force constant of the atom bonded to the backbone are wrong, which might

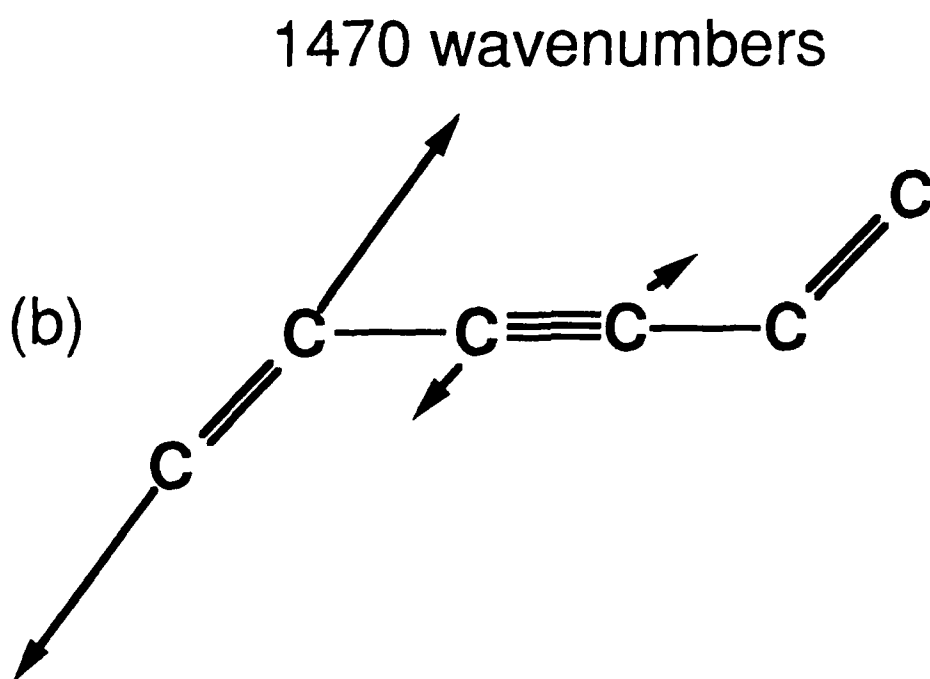
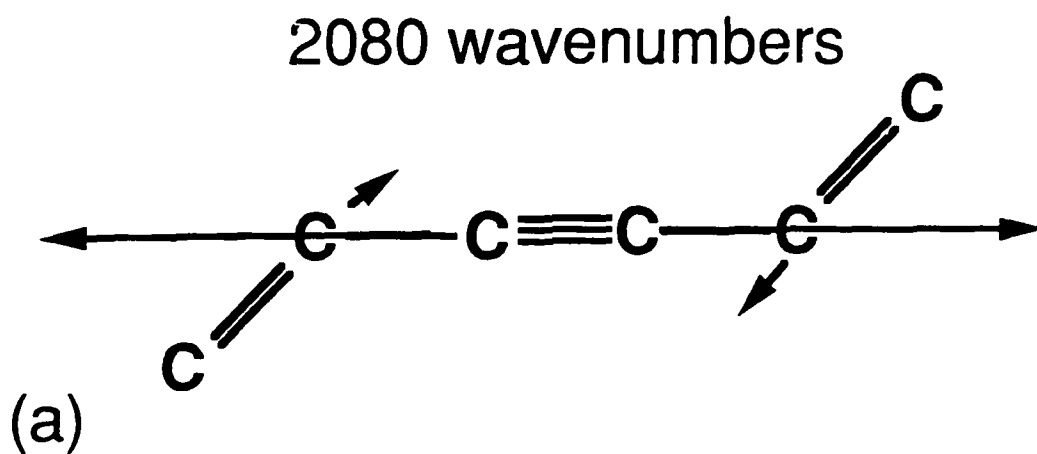


**Figure 21.** Eigenvectors for the two PDA Raman active backbone vibrational modes whose frequency shifts are investigated in this study

affect the vibrational coupling to the backbone. This possibility was investigated by performing a frequency calculation on PDA with methyl substituents, which gives the C-C bond to the backbone found in all the PDA derivatives, but changing the mass of the carbon atom on the methyl group to 32 amu. The backbone frequencies described before did not change. This was a useful result for this study because the calculation time for a methyl substituted PDA cluster is very much longer than hydrogen substituted PDA because the methyl substituted cluster has 27 more (hydrogen) atoms.

The strain dependent frequency shift of the backbone frequency corresponding the mode shown in figure 21a is shown in figure 22. Because a four repeat unit cluster was used in the calculation, there are four frequencies in the cluster which correspond to the vibrational mode in the infinite chain. The difference in these frequencies is very small, which shows that they are nearly degenerate. The calculated frequency shift as a function of strain shows more spread than the PE results, which is a limitation of the accuracy in calculating the frequencies on such a large cluster. The calculated strain dependent frequency shift of this mode is  $40 \pm 3 \text{ cm}^{-1} / \% \text{ strain}$ , which is the average of the four lines. The experimental value of the frequency shift varies, but the largest reported is  $20 \pm 0.5 \text{ cm}^{-1} / \% \text{ strain}$ .<sup>32</sup> The experiment that measured the largest shift was performed on PDA samples with best morphologies, which implies that this shift is more representative of the defect free crystal. Galliotis et al<sup>21</sup> list a number of measured values for the shift of two backbone Raman active modes for a range of PDA derivatives of varying quality, which gives

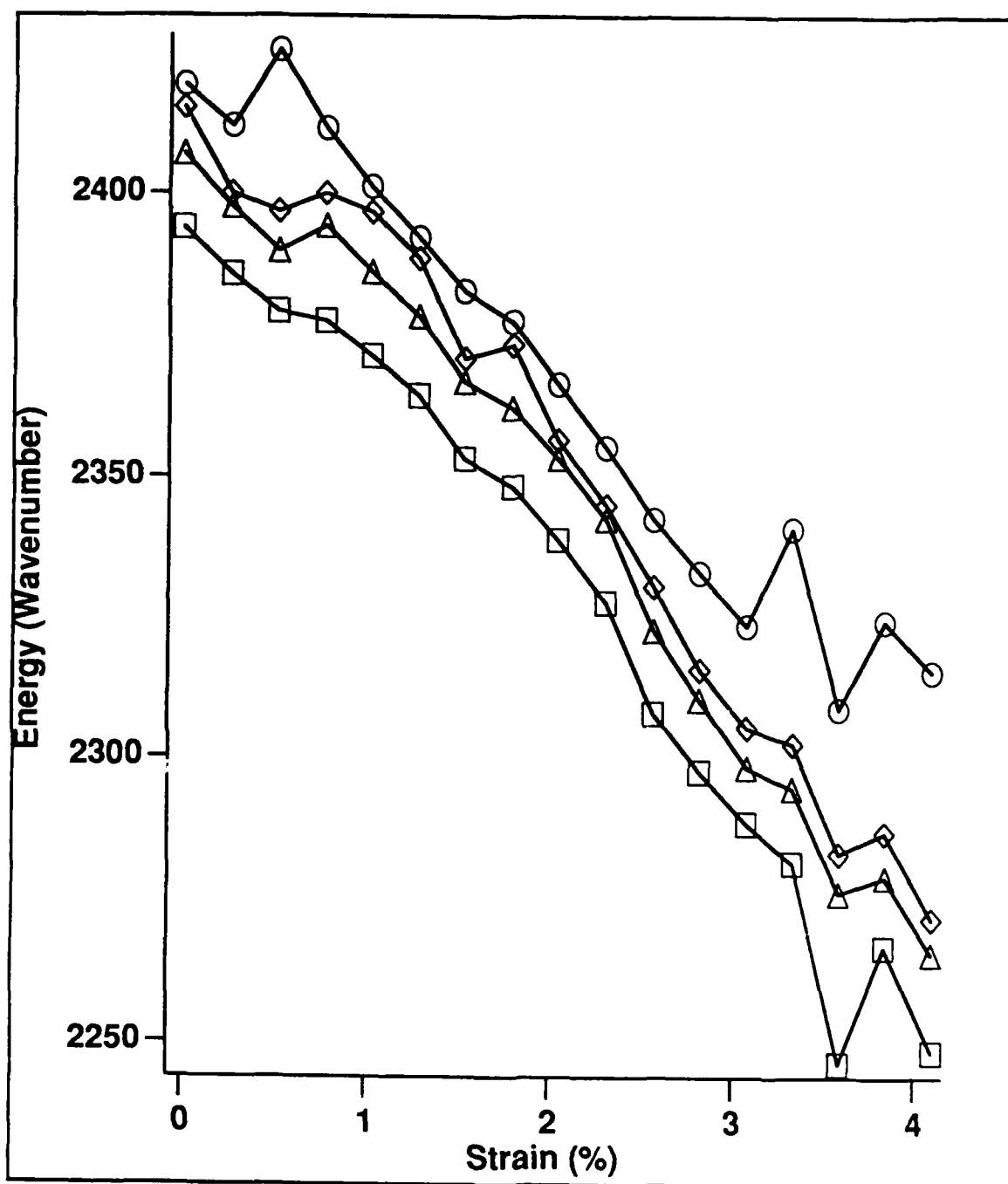


**Figure 22.** Strain dependent frequency shifts of the 4 repeat unit PDA cluster corresponding to the vibrational mode shown in figure 20 (a).

an idea of the sensitivity of these shifts to sample preparation. As was found for PE, the calculated frequency shift of this mode is approximately twice that observed experimentally.

The frequency shift of the mode shown in figure 21b is shown in figure 23. There are only 3 frequencies in the 4 repeat unit cluster for this mode because it involves displacement of the carbons along the double bonds, and there are only 3 double bonds in the cluster. There is considerable spread in these calculated strain dependent frequencies; however, the average calculated frequency shift of this mode is  $15 \text{ cm}^{-1} / \% \text{ strain}$ , which is approximately twice the highest reported value for the shift of this mode<sup>15</sup>.

As was the case for PE, it would be informative to compare the potentials generated by AM1 for the individual bonds in PDA with Morse potentials; however, Morse potential parameters have not been reported for these bonds. Because the electrons are not localized to specific atom pairs in PDA, it is more difficult to define potentials that accurately describe the interaction. The AM1 potentials for the single, double, and triple C-C bonds in PDA are shown in Figure 24. These potentials are best described by third order polynomials, which are stiffer than Morse potentials. Instead of explicitly defining a bond potentials, empirical force constant approaches for calculating the modulus in various PDA derivatives obtain set of force constants from the equilibrium spectrum, and use a fudge factor to describe the variation of the force constant with strain. An empirically derived



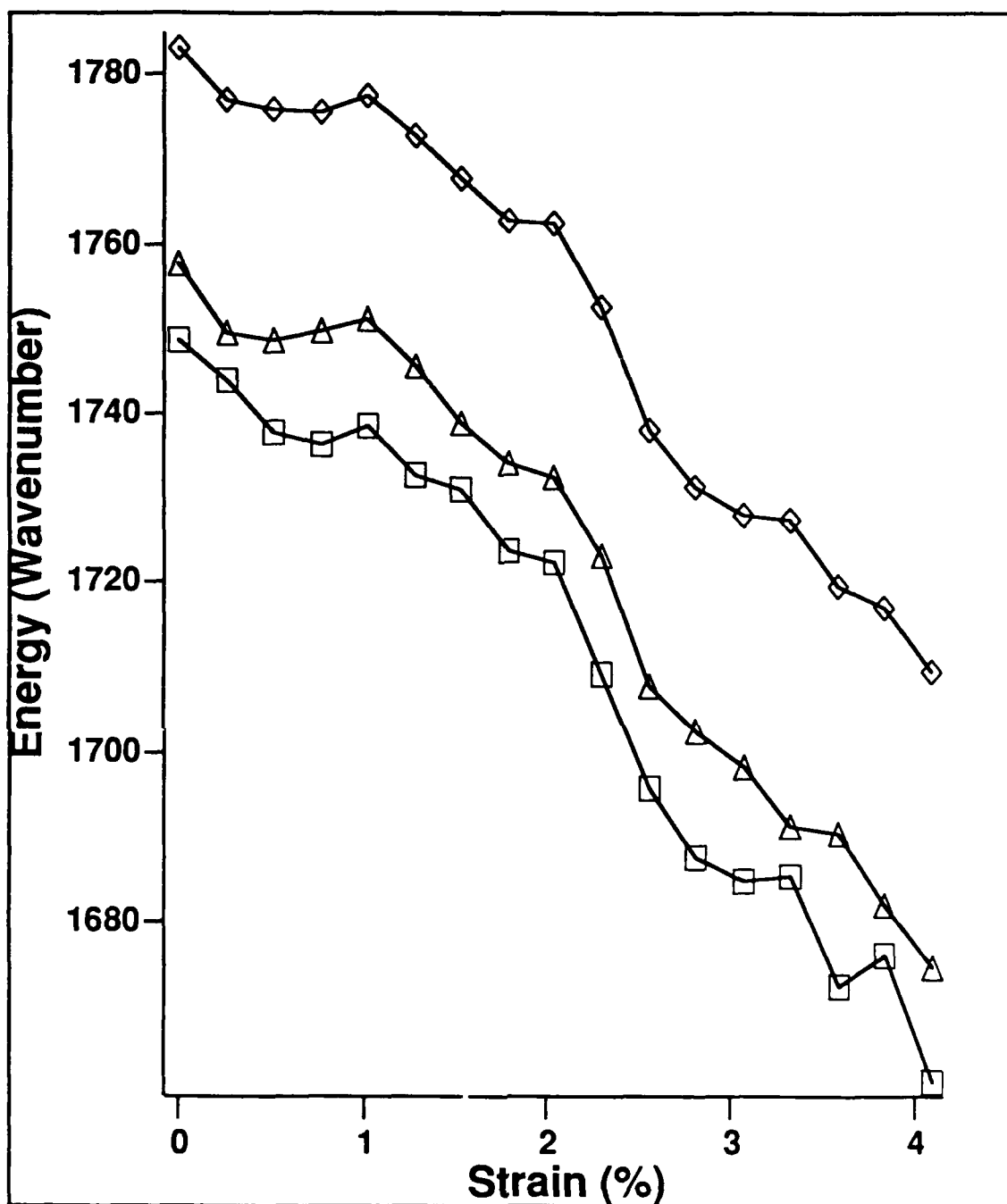


**Figure 23.** Strain dependent frequency shifts of the 4 repeat unit PDA cluster corresponding to the vibrational mode shown in figure 20 (b).

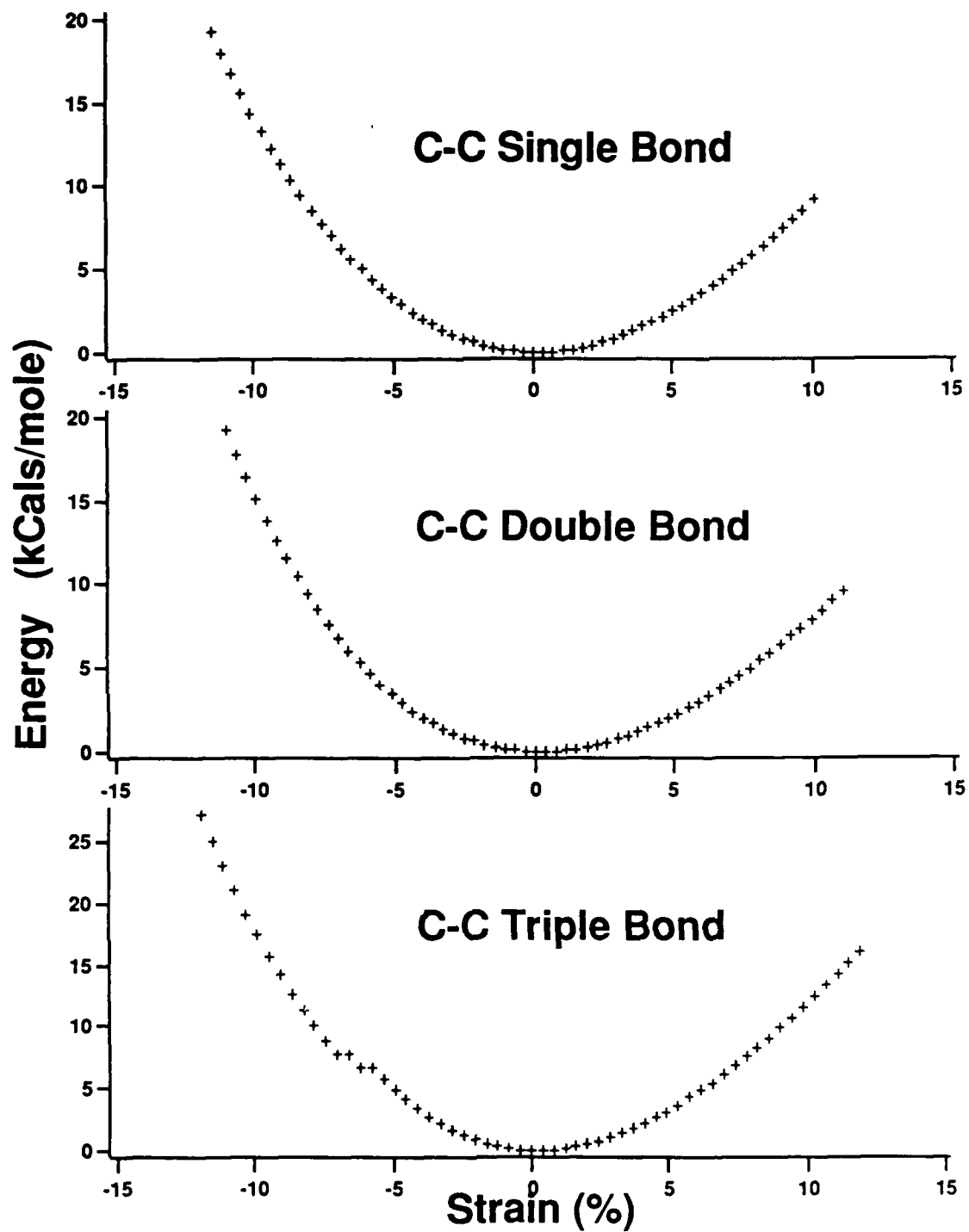


**Figure 24.** Comparison of PDA C-C bond potentials

estimate of the force constant variation is <sup>33,34</sup>

$$k = \frac{B}{r-A} \quad (14)$$

where  $A=1.06 \text{ \AA}$  and  $B = 1.65 \times 10^{-8} \text{ Nt}$ . This approximate relation is known to overpredict the strain dependent frequency shift, which is not surprising because it predicts the force constant to fall off as  $1/r$ , which is slower than the force constant variation of a Morse potential. An accurate calculation of the strain dependent frequency shift in PDA has not been reported.

A comparison of the equilibrium force constants obtained from the second derivatives of the AM1 potentials shown in Fig 24 and those reported in by Batchelder and Wu is shown in Table 8. As is seen, the AM1 values for the force constants are considerably higher than those derived from the PDA spectra. The models from which these PDA experimental force constants were derived were simplified, so these force constants are not guaranteed to be unique. Also listed in Table 8 are the force constants for the corresponding unconjugated C-C bonds calculated by AM1. The force constants for the unconjugated bonds are in a ratio which is close to 1:2:3 for single to double to triple, while in PDA the single and double have roughly equal strength, each approximately one-half that of the triple bond.

TABLE 8

## COMPARISON OF PDA BACKBONE FORCE CONSTANTS [Nt/m]

C-C Bond Type	AM1	Ref 29	Ref 30	AM1 Unconjugated
Single	820	450	560	620 (C <sub>2</sub> H <sub>6</sub> )
Double	880	550	510	1220 (C <sub>2</sub> H <sub>4</sub> )
Triple	1530	1200	1170	1880 (C <sub>2</sub> H <sub>2</sub> )

The deformation of PDA does not involve only one kind of bond, so a comparison of the individual calculated and experimental force constants does not have a direct correlation to the error of the calculated modulus. However, as a rough comparison, using a simple addition of the bonds found in the repeat unit, two single C-C, one double C-C, and one triple C-C, bond, the AM1 calculated sum is approximately 40% higher than experiment. Because the deformation analysis showed that the change of the bond angle contributed more to extension along the *c*-axis than bond extension, the overestimate of the modulus is less than the 40% overestimate of the bond stiffnesses.

## VI SUMMARY, CONCLUSIONS, AND RECOMMENDATIONS

The ultimate mechanical properties of polymers, assuming perfect morphology, will be limited by the mechanical properties of a single, ideal chain. The standard approach used to predict the chain moduli of polymers, the ubiquitous method of Treolar<sup>41</sup>, uses force constants for bond stretching, bond angle opening, and torsion angle twisting, obtained from spectroscopy to build up a classical mechanics model of the polymer as a series/parallel combination of ideal springs. Extensions to this approach incorporate strain dependence (anharmonicity) in the force constants (ref 35, 36 for example). While the method of Treolar has the advantage of being grounded in experiment, it is inconvenient to apply in many situations because polymer spectra tend to be complex, making the task of unambiguously obtaining the required force constants very difficult. In addition, the method of Treolar can only be applied to polymers which have already been synthesized, i.e., it provides no predictive capability for designing polymers with desirable mechanical properties. Likewise, molecular mechanics is based on situation specific experimental data, and has a limited predictive capability.

SE quantum mechanical calculations of polymer mechanical properties were attempted because the SE method is generic enough to have a predictive capability, and ab-initio methods at present are too time consuming to be practical for polymers. Moduli values obtained were systematically (and significantly) higher than experimental values, which was attributed to morphological imperfections which will be present in any

real material. The goal of this investigation was to explore possible inaccuracies inherent in the SE method which would contribute to these discrepancies. The criterion used to make this assessment was the strain dependent behavior of polymer spectra and strain potentials of individual bonds within the polymers PE and PDA, polymers which have been well characterized experimentally and have relatively simple structures.

At the beginning of this investigation it was anticipated that the SE method would be valid for some small region around equilibrium (whose range would be bounded in this investigation) but would be invalid above (and below) some critical value of strain. This anticipation was based on the fact that the SE method used in the calculation (as well as most SE methods) was parameterized to reproduce equilibrium molecular properties. Almost any physically realistic molecular potential is nearly harmonic around equilibrium (harmonic approximation of an anharmonic oscillator) so the extrapolation of equilibrium properties for small deviations around equilibrium is valid. What was found in this investigation is that the force constants obtained from the SE method, even at equilibrium, are too high. The individual strain dependent bond potentials produced by the SE method were found to be significantly stiffer than Morse potentials used to describe these bonds; the Morse potentials used in the comparison have been shown to accurately describe the anharmonicity and reproduce strain dependent spectral shifts in PE.<sup>17</sup> As a group, the SE generated potentials were found to be well fit by cubic potentials, which is essentially a first order correction to a harmonic

potential. Because a polymer has many deformation modes, the overprediction of bond stiffness is not necessarily equal to the overprediction of polymer modulus.

The consequences of the SE prediction of bond potentials is illustrated in Figure 25. Figure 25a shows a comparison of Morse, harmonic, and cubic potentials which have been constructed to have the same second derivative at equilibrium. The Morse potential is the C-C potential from Wool<sup>17</sup>; the harmonic and cubic potentials are least squares fits to this Morse potential. Figure 25b shows the first derivative of these potentials, which is the molecular stress-strain curve. Figure 25c shows the second derivative of these curves, which has the same shape as the modulus curve for this potential because the second derivative and modulus differ only by constants. The second derivative of the harmonic curve is a constant; an ideal harmonic material would have a modulus which is independent of strain (and would never fracture). If the bond is accurately described by a cubic potential, the modulus linearly decreases with tension and increases with compression. The second derivative of the Morse potential initially decreases faster in tension than the cubic, and falls off slower at strains above 15%. The Morse potential's second derivative increases faster than the cubic in compression. However, for small values around equilibrium, the second derivative of the Morse potential can be well described by a linear fit, so it could be difficult to discriminate between Morse and cubic potentials since experiments are limited to small strains (by bulk failure mechanisms).

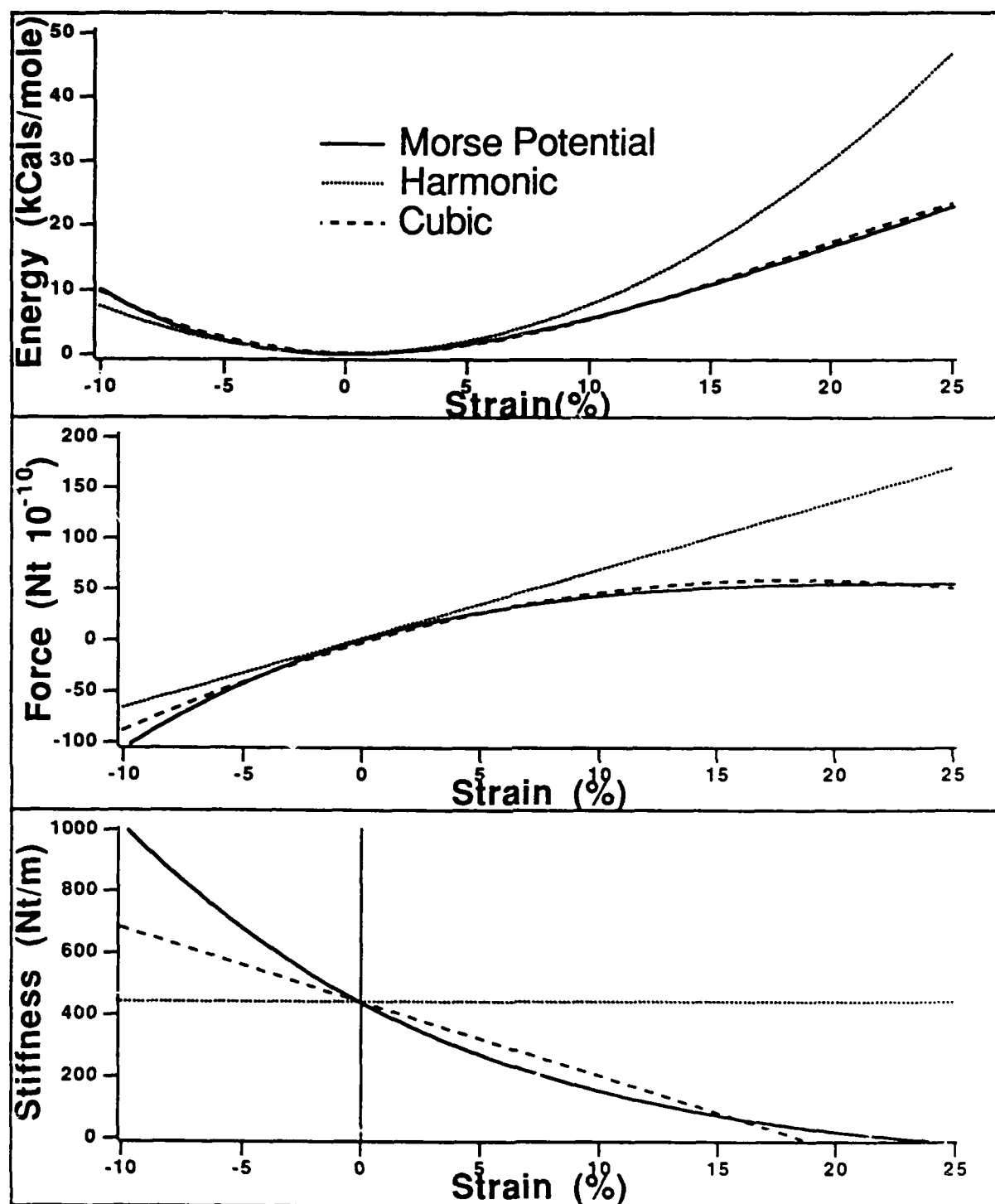


**Figure 25.** Comparison of Morse, Harmonic, and Cubic potentials (a), the force curves (b), and the stiffness curves (c) from each. These potentials were constrained to have equal second derivatives at equilibrium.



What are the possible reasons for the observed behavior of the SE method? First, the SE method was not parameterized with data that give information about the derivatives of the molecular potentials, even at equilibrium. Thus the inaccuracy of the predicted stiffness away from equilibrium is not surprising. A more basic limitation may be the fact that SE methods are subject to the Hartree-Fock limit. It is necessary to include electron correlation in ab-initio calculations to obtain good agreement with experimental spectra, i.e., derivatives of the molecular bond potentials.<sup>6</sup> Electron correlation is known to reduce bond stiffness; bonds calculated at the Hartree-Fock limit are found to be systematically stiffer than experiment, which is consistent with the results of the SE calculations performed in this investigation. Since mechanical properties of polymers ultimately depend on derivatives of the molecular bond potentials, the accuracy of a calculation of polymer chain modulus can be judged on the basis of the method's ability to match these derivatives on systems where experimental data exists.

SE calculations produce usefully accurate results for those properties against which they have been benchmarked; the AM1 parameterization did not include the spectroscopic information which would give better values for the equilibrium force constant and a more accurate description of the behavior of the system away from equilibrium. For the foreseeable future, ab-initio methods will remain too computationally expensive to be practical for the prediction of the mechanical properties of polymers. In order to improve the SE calculations of mechanical properties of polymers, one can

parameterize the method to reproduce spectroscopic data, which will give a better anchor for bond stiffness. Scaling procedures to improve force constants calculated at the Hartree-Fock limit have been developed for some situations.<sup>9</sup> It may be possible to incorporate a similar procedure in a SE parameterization, and avoid the computational cost of ab-initio methods. An extensive parameterization could be avoided because nearly all polymers of interest contain only carbon, hydrogen, oxygen, nitrogen, sulfur, and phosphorous, which would reduce the cost of such an effort.

The synthesis to high molecular weight (long chains), purification, and processing of a new polymer is a long and expensive process. The accurate computational prediction of the ultimate mechanical (and other) properties of polymers is a desirable goal because it can provide guidance on which new polymers possess the best potential for high modulus and strength.

## REFERENCES

1. H. E. Klei, J. J. P. Stewart, New Polym. Materials, Int. J. Quant. Chem, Quant. Chem. Symp., **20**, 529 (1986).
2. S. G. Wierschke, AFWAL-TR-88-4201 (October 1988).
3. H. Bethe and E. Salpeter, *Quantum Mechanics of One and Two Electron Atoms*, (Plenum Publishing Corp, New York, 1977).
4. J. A. Pople and D. L. Beveridge, *Approximate Molecular Orbital Theory*, (McGraw-Hill, New York, 1970).
5. P. W. Atkins, *Molecular Quantum Mechanics*, (Oxford University Press, Oxford, 1983).
6. A. Szabo and N. S. Ostlund, *Modern Quantum Chemistry*, (MacMillan, New York, 1982).
7. V. Fock, Z. Physik, **61**, 126 (1930).
8. D. R. Hartree, Proc. Cambridge Phil. Soc., **24**, 89 (1928).
9. V. I. Pupyshev, Y. N. Panchenko , and G. Pongor , J. Chem. Phys. **94**, 1247 (1991).
10. W. Meyer and P. Rosmus, J. Chem. Phys, **63**, 2356 (1975).
11. J. A. Pople, D. P. Santry, and G. A. Segal, J. Chem. Phys., **43**, S129 (1965).
12. T. Clark, *A Handbook of Computational Chemistry*, (John Wiley and Sons, New York 1985).
13. M. J. S. Dewar, E. G. Zoebisch, E. F. Healy, and J. J. P. Stewart, J. Am. Chem. Soc, **107**, 3902 (1985).
14. J. J. P. Stewart, J. Comp. Chem., **10**, 221 (1989).
15. P. G. Perkins, J. J. P. Stewart, J. C. S. Faraday II, **76**, 520 (1980).
16. J. J. P. Stewart, FJSRL-TR-88-0007 (December 1988).
17. Gaussian 90, Revision F, M. J. Frisch, M. Head-Gordon, G. w. Trucks, J. B. Foresman, H. B. Schlegel, K. Raghavachari, M. Robb, J. S. Binkley, C. Gonzalez, D. J. Defrees, D. J. Fox, R. A. Whiteside, R. Seeger, C. F. Melius, J. Baker, R. L. Martin, L. R. Kahn, J. J. P. Stewart, and J. A.

Pople, Gaussian, Inc., Poittsburgh, PA, 1990. Gaussian88 is an earlier version of this program.

18. P. M. Morse, *Phys Rev*, **34**, 57 (1929).
19. R. P. Wool and R. S. Bretzlaff, *J. Polym. Sci. B, Polym. Phys. Ed.*, **24**, 1039, (1986).
20. S. Flügge, *Practical Quantum Mechanics*, (Springer-Verlag, Berlin 1974).
21. C. Galliotis and R. J. Young, *Polymer*, **24**, 1023 (1983).
22. R. J. Young, *Introduction to Polymers*, (Chapman and Hall, London 1981).
23. L. Holliday in *Structure and Properties of Oriented Polymers*, edited by I. M. Ward, (Wiley, New York 1975).
24. H. Tadokora, *Structure of Crystalline Polymers*, (Wiley, New York 1979).
25. S. Kumar and T. E. Helminiak, in *The Material Science and Engineering of Rigid-Rod Polymers*, ed. by W. W. Adams, R. K. Eby,, and D. E. McLemore, (Materials Research Society, Pittsburg PA 1988).
26. B. Crist, M.A. Ratner, A. L. Brower, and J. R. Sabin, *J. Appl. Phys.*, **50**, 6047 (1980).
27. R. P. Wool, R. H. Boyd, *J. Appl. Phys.*, **51**, 5116, (1980).
28. R. G. Snyder and J. H. Schachtschneider, *Spectrochimica Acta*, **19**, 85, (1963).
29. J. H. Schachtschneider and R. G. Snyder, *Spectrochimica Acta*, **19**, 117 (1963).
30. Cerius Version 2.1, Cambridge Molecular Design, 1990.
31. W. W. Adams, *An Electron Microscopy and X-Ray Scattering Investigation of the Deformation Morphology of Solid State Extruded Fibers and Melt Draw Films of Polyethylene*, PhD Dissertation, University of Massachusetts (1984).
32. C. Galliotis and R. J. Young, *Polymer* **24**, 1023 (1983).
33. A. C. Cottle, W. F. Lewis, and B. N. Batchelder, *J. Phys. C: Solid State*

Physics, **11**, 605 (1978).

34. W. F. Lewis and B. N. Batchelder, Chem. Phys. Lett., **60**,232, (1979).

35. B. N. Batchelder and D. Bloor, J. Polym. Sci., Polym. Phys. Edn., **17**, 569, (1979).

36. G. Wu, K. Tashiro, and M. Kobayashi, Macromolecules **22**, 188 (1989).

37. V. Enkleman and G. Schleir, Acta Crys., **B36**, 1954 (1980).

38. H. Eckhardt, D. S. Boudreaux, and R. R. Chance, J. Chem. Phys **85**, 4116, (1986).

39. V. M. Mitra and W. M. Risen, J. Chem. Phys, **66**, 2731 (1977).

40. C. Galiotis, R. J. Young, and D. N. Batchelder, J. Polym. Sci.: Polym. Phys. Edn., **21**, 2483 (1983).

41. L. R. G. Treolar, Polymer **1**, 95 (1960) and references therein.

## Vita

Captain James R. Shoemaker was born on 30 August 1963 in Aurora, Illinois. After graduating from Marmion Military Academy, he attended the University of Illinois at Urbana-Champaign, receiving a Bachelor of Science degree in Engineering Physics and a commission in the USAF in December 1984. He served as a Research Physicist in the Plasma Physics Group, Aero Propulsion and Power Laboratory , Wright Patterson AFB., with his research concentrating on Rydberg state Stark spectroscopy of helium. He entered the School of Engineering, Air Force Institute of technology in August 1989.

REPORT DOCUMENTATION PAGE			Form Approved OMB No. 0704-0188	
Public reporting burden for this collection of information is estimated to average 1 hour per response, including the time for reviewing instructions, searching existing data sources, gathering and maintaining the data needed, and completing and reviewing the collection of information. Send comments regarding this burden estimate or any other aspect of this collection of information, including suggestions for reducing this burden, to Washington Headquarters Services, Directorate for Information Operations and Reports, 1215 Jefferson Davis Highway, Suite 1204, Arlington, VA 22202-4302, and to the Office of Management and Budget, Paperwork Reduction Project (0704-0188), Washington, DC 20503.				
1. AGENCY USE ONLY (Leave blank)		2. REPORT DATE March 1991	3. REPORT TYPE AND DATES COVERED Master's Thesis	
4. TITLE AND SUBTITLE AN ASSESSMENT OF THE ACCURACY OF SEMI-EMPIRICAL QUANTUM CHEMISTRY CALCULATIONS OF THE MECHANICAL PROPERTIES OF POLYMERS			5. FUNDING NUMBERS	
6. AUTHOR(S) Captain James R. Shoemaker, USAF				
7. PERFORMING ORGANIZATION NAME(S) AND ADDRESS(ES) Air Force Institute of Technology, WPAFB OH 45433-6583			8. PERFORMING ORGANIZATION REPORT NUMBER AFIT/ENP/GNE/91M-9	
9. SPONSORING / MONITORING AGENCY NAME(S) AND ADDRESS(ES)			10. SPONSORING / MONITORING AGENCY REPORT NUMBER	
11. SUPPLEMENTARY NOTES				
12a. DISTRIBUTION / AVAILABILITY STATEMENT Approved for public release; distribution unlimited.			12b. DISTRIBUTION CODE	
13. ABSTRACT (Maximum 200 words) The ultimate mechanical properties of polymers, assuming perfect morphology, will be limited by the mechanical properties of a single, ideal polymer chain. Previous calculations of polymer chain moduli using semi-empirical (SE) quantum chemistry methods have resulted in modulus values much higher than experimentally measured. This study investigated the error in the calculated inherent to the method of calculation by comparing SE results for C-C bond potentials in two well characterized polymers, polyethylene and polydiacetylene. It was found that the SE calculation systematically overpredicted bond stiffness in these polymers by approximately 25% to 30%. This is the upper limit on the modulus overprediction, depending on the importance of bond extension/compression (as compared to other deformation modes) in the overall deformation of the polymer chain. It is believed that this discrepancy is caused in part by the omission of bond stiffness information in the parameterization of the SE method, and in part by the omission of electron correlation in the calculation (Hartree-Fock Limit).				
14. SUBJECT TERMS Polymer Modulus, Quantum Chemistry, Spectroscopy			15. NUMBER OF PAGES 100	
			16. PRICE CODE	
17. SECURITY CLASSIFICATION OF REPORT Unclassified	18. SECURITY CLASSIFICATION OF THIS PAGE Unclassified	19. SECURITY CLASSIFICATION OF ABSTRACT Unclassified	20. LIMITATION OF ABSTRACT UL	